HERIOT WATT UNIVERSITY

MPHIL THESIS

Adaptive Waveform Design for Cognitive Radar

Author:
Georgios TSISTRAKIS

Supervisor:
Dr. Mathini SELLATHURAI

A thesis submitted in fulfilment of the requirements
for the degree of Master of Philosophy
in the
School of Engineering and Physical Sciences

December 2014

HERIOT WATT UNIVERSITY

Abstract

School of Engineering and Physical Sciences

Master of Philosophy

Adaptive Waveform Design
for Cognitive Radar

by Georgios TSISTRAKIS

Advances in technology, especially in sensing, robotics, wireless communications, hardware capabilities and the constant need to confront not only the existing but also new and advanced threats are pushing for the need of advanced radar techniques. In this context, Cognitive Radar (CR) is visualized as the next generation multifunctional, smart and adaptive radar that extends its capabilities and responsibilities far beyond the traditional radar. CR incorporates knowledge gained by the interaction with the environment into its operation therefore forming a closed-loop system aiming to enhance the system performance. A very important element of the CR operation is the ability to adaptively design the transmitted waveforms based on the radar objective and the changes in the environment. In this thesis, we present the different aspects involved in the Cognitive Radar concept with deeper focus on the adaptive waveform design of the system aiming to improve the tracking performance. A method of adaptive waveform design within the sensor management problem ensuring that the total transmitted power is reduced compared to the transmission of a fixed waveform is proposed and finally a promising direction towards the multi-sensor resource allocation and waveform design is presented.

Contents

Abstract i

Contents ii

List of Figures iv

Symbols vi

1 Introduction 1
- 1.1 Background and Motivation . . . 1
- 1.2 Overview . . . 8

2 Adaptive Waveform Design 10
- 2.1 Introduction and Objectives . . . 10
- 2.2 Echo-location System of Bats . . . 11
- 2.3 Waveform Design Literature Review . . . 17
  - 2.3.1 Nature Inspired . . . 18
  - 2.3.2 Arbitrary Waveform Design . . . 19
  - 2.3.3 Probability Density Function Distance . . . 20
  - 2.3.4 Information Theoretic Approach . . . 21
  - 2.3.5 Control Theoretic Approach . . . 22
- 2.4 Adaptive LFM Waveform . . . 28
  - 2.4.1 Overview of Tracking Algorithms . . . 30
- 2.5 Library of Adaptive Waveforms and Collaboration Strategy . . . 33
- 2.6 Summary and Conclusions . . . 39

3 Adaptive Waveform Design under Power Constraints for Search and Track 41
- 3.1 Introduction and Objectives . . . 41
- 3.2 Sensor Management and Adaptive Waveform Design . . . 43
  - 3.2.1 Track Mode . . . 44
  - 3.2.2 Search Mode . . . 47
- 3.3 Implementation and Results . . . 49

3.4 Summary and Conclusions 53

4 Multi-Sensor Resource Allocation and Waveform Design 56
4.1 Introduction and Objectives 56
4.2 Resource Allocation Literature Review 57
4.3 Joint Framework for Resource Allocation and Waveform Design 59
4.4 Summary and Conclusions 65

5 Conclusions and Further Work 66

A Radar Fundamentals 69
A.1 Unambiguous Range and the Radar Equation 69
A.2 Range Resolution and Doppler Effect 70
A.3 Radar Waveforms 70

B Ambiguity Function 75
B.1 Main Properties of the Ambiguity Function 76
B.2 Examples of the Ambiguity Function 76

Bibliography 82

List of Figures

1.1 Pulsed radar operating principle. 2
1.2 Block Diagram of Cognitive Radar. 5

2.1 [1] Echolocation tasks of bats during spatial orientation (a) and search for prey (b) in different habitats. The emitted pulse and the echo returning from prey (grey) are displayed together with echo trains from background targets (white). 12
2.2 [2] Spectrograms of sonar signals produced by four different species of bats as they search and pursuit insects. 13
2.3 Radar/aircraft geometry. 14
2.4 Range resolution vs Pulse Bandwidth. 15
2.5 SNR of different pulse bandwidth. 16
2.6 Maximum Unambiguous Range vs PRF. 16
2.7 The variety of approaches and tools used in adaptive waveform design. . . . 18
2.8 Mean square error of fixed and adaptive waveforms. 29
2.9 Mean square error of Kalman Vs Cubature Kalman filters. 32
2.10 Block diagram of proposed collaborative strategy. 36
2.11 Tracking Error of Fixed vs Adaptive Waveform. 37
2.12 Pulse Duration of Adaptive Waveform. 37
2.13 Waveform Class Selection. 38
2.14 Mean Error of Collaborative vs non-Collaborative strategy. 39

3.1 P_d as a function of SNR_{dB} for $P_{fa} = 10^{-6}$. 46
3.2 Targets in surveillance area. The dotted line represents the range where the probability of detection is $P_d = 0.5$ (blue for fixed, red for adaptive waveform when $T_k^* = T_{max}$). The initial position of the targets is represented by the blue squares (existing targets) and circles (arrived during the simulation). The line next to them represents their trajectory. 52
3.3 Cell illuminations. Blue square for search mode and red circles for track. The asterisk denotes that one or more new targets have been detected. . . . 52
3.4 Total Power saved by the adaptive waveform, normalized to the power of a fixed pulse with $T_f = 0.3sec \cdot 10^{-5}$. 53
3.5 Mean P_d per target for adaptive vs fixed waveform. 54
3.6 Mean tracking error per target. 54

A.1 LMF Waveform. 71

A.2 Frequency assignment in a Costas code of length 10. 72
A.3 List of Barker Codes. 73
A.4 Coherent pulse train of N=5. 73

B.1 Ideal Ambiguity Function. 77
B.2 3-D plot of the single pulse Ambiguity Function. 77
B.3 Contour plot of the single pulse Ambiguity Function. 78
B.4 3-D plot of the LFM single pulse Ambiguity Function. 79
B.5 Contour plot of the LFM single pulse Ambiguity Function. 80
B.6 3-D plot of the LFM Coherent Train of Pulses Ambiguity Function. 81
B.7 Contour plot of the LFM Coherent Train of Pulses Ambiguity Function. . . 81

Symbols

t	time
f_c	carrier frequency
T	pulse duration
T_{PRI}	pulse repetition interval
r	target range
v	target velocity
c	speed of light
B	pulse bandwidth
b	radar cross section (RCS)
F_n	noise figure
L_r	receiver loss
G	antenna gain
P_t	peak power
s	signal
n	signal-to-noise ratio (SNR)
T_e	effective noise temperature
V	measurement noise vector
R	measurement noise covariance matrix
P	state estimation covariance matrix
W	process noise vector
Q	process noise covariance matrix
$\mathbf{I}$	mutual information
X	target state

Symbols

Y	radar measurements
k	time step
f	transition function
F	transition matrix
h	transformation function
H	transformation matrix
p	probability density function
K	Kalman gain
$\mathbf{E}$	expected value
J	Fisher matrix
w	weight
m_i	beam
Δn_m	beam width
A_i	cell
P_d	probability of detection
P_f	probability of false alarm
$\mathcal{H}$	entropy
e	Euler's number
a	path loss
R_u	maximum unambiguous range
P_r	received power
P_{ref}	reflected power
P_{th}	receiver power threshold
π	pi constant
τ	signal trip time
λ	wavelength
Λ	expected undetected targets
θ	waveform parameters
ω	Doppler frequency
μ	chirp rate

Symbols

μ^{A_i}	target arrival rate
Γ	track to track&search desired ratio
γ	track to track&search real ratio
χ	ambiguity function

HERIOT WATT UNIVERSITY

Abstract

School of Engineering and Physical Sciences

Master of Philosophy

Adaptive Waveform Design
for Cognitive Radar

by Georgios TSISTRAKIS

Chapter 1

Introduction

1.1 Background and Motivation

Radars are electromagnetic systems that are used to detect and track targets. The operating principles of radar systems are relied on the transmission of a signal and the reception of its reflections from different objects that are illuminated by the transmitted signal. Due to the fact that the detection of the objects is done by using transmission from the same system, radars are called 'active sensors'. In comparison, human vision and hearing are passive systems. Passive electromagnetic systems that detect targets have also been developed [3] [4] [5]. The main advantage of radars compared to passive systems is that they can measure objects distance immediately. It is important to note that active sensors can be found in nature only in a few living organisms, like the bats and some species of aquatic mammals [2]. Today's radar systems technology uses electromagnetic spectrum starting from VHF (100 MHz) and extends up to EHF (100GHz). Low frequencies of this spectrum are affected slightly by the atmospheric conditions, so the visibility provided by these radars in terms of detection range is much larger compared to the human vision. On the other hand, there are occasions where the human eye can outperform even the most complex radar system in terms of detection, tracking and identification performance and executes these tasks faster and more reliable.

A radar system is composed by the following three main subsystems:

- Transmitter, where the transmitted signal is generated and emitted to the environment.
- Receiver, where the returns of the transmitted signals are collected.
- Processor and Monitor, where the received signals are analysed and the results are displayed.

In fig.1.1 we can see a simple pulsed radar diagram, where the radar operating (carrier) frequency is f_c, the signal is a sinusoidal pulse with duration T and the pulses are repeated every T_{PRI} seconds. Pulse Repetition Frequency is defined as $PRF = 1/T_{PRI}$. The transmitted signals reflect in the targets they encounter and a portion of the signals' power returns to the antenna as echo. The time it takes a pulse to travel the two-way path between the radar and the target is $\tau = 2r/c$, where r is the distance of the target and c is the speed of light. By measuring time τ we can directly compute the distance r.

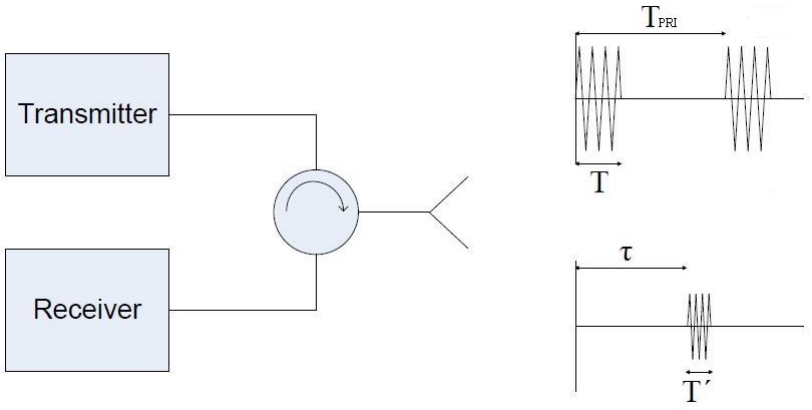

FIGURE 1.1: Pulsed radar operating principle.

Appendix A provides a short presentation of the fundamental principles and theory of radar operation which are useful for the work in the thesis.

Nowadays the radar environment becomes more and more complex and the radar usually has to cope with more than one target, targets that try to hide themselves from radars in clever ways and operate in difficult environments with high noise. Recent advances in technology and especially in the radar and sensing technology have created a demand for new capabilities on the modern radars, utilizing technologies like knowledge-based waveforms, data processing, waveform adaptivity through diversity, machine learning etc. Modern

radars can use all of the above techniques to improve their performance, even on aged electronics and radar hardware, adapting the radar's algorithm on the continuously changing environment. Modern high performance radars require diverse waveform design in order to achieve their missions such as detecting moving targets, imaging terrain and measuring accurately range, angle and Doppler. Radar hardware developments, like digital arbitrary waveforms generators and advances in computational capability that allow algorithms to design both modulus and phase of a waveform, have allowed radars to interact with the environment in a smart way. The concept of the next generation multifunctional and smart radar was proposed in [6] where sensors and platforms were visualized embodied with artificial intelligence. Unlike traditional radars that are calibrated to operate under certain specifications with fixed operating parameters regardless of the dynamic environment, the next generation radars are equipped with the ability to adaptively alter their algorithms and waveforms. Studies have shown that challenges similar to the ones of such radars have been adequately overtaken by the visual brain and the study of it can give us the knowledge and the ideas needed to evolve radars into 'smart' and 'thinking' radars [7]. What radars should mimic is the concept of cognition and a definition of cognition is given in [8]:

"Conscious mental activity that informs a person about his or her environment. Cognitive actions include perceiving, thinking, reasoning, judging, problem solving, and remembering."

Of course, all of the above properties refer to human but we can still map them into equivalent real engineering systems.

- The human property of perceiving is translated to sensing.
- Thinking, reasoning, judging and problem solving can be mapped to expert systems, rule-based reasoning, adaptive algorithms and computation.
- Lastly, remembering means that the radar should have memory and keep a database with the environmental information.

In this context, the next step in this evolution of dynamic radars is commonly described as Cognitive Radars (CR) [9]. CR has sensors and algorithms that autonomously adapt to their environment and the waveform parameters dynamically change in order to match the

characteristics of the target and the mission of the radar. An information feedback loop from the receiver to the transmitter is the most important step towards achieving that. In order to cope with the latest challenges important qualities that CR incorporates are the abilities of awareness, storage and reasoning. These systems have the ability to monitor the environment on which they operate and adapt to it, meaning they have to decide what to transmit and how to process the returns. It is well known that the used waveforms highly affect the tracking error [10].

One of the aims of Cognitive radar is to select the best sequence of waveforms to achieve the highest possible accuracy in target tracking restricted by the fact that a waveform can have high range resolution or Doppler resolution but not both at the same time. The dynamic waveform selection for target tracking systems was first studied in [11], where Kalman filter and waveforms with linear time-frequency characteristics were used. A simple way to perform waveform adaptivity is to define a cost function that will specify the cost of tracking a target and will choose the appropriate waveform that will optimize this function for every pulse emitted. This approach makes it possible to improve the performance of the radar compared to the fixed waveforms radars. Pulse-to-pulse waveform agility provides many opportunities and degrees of freedom for improved performance and efficiency. In every transmission, the transmitted waveform is adaptively updated based on the radar's objectives, previous measurements and priori information. However, other researches [12] support that more improvement can be earned by making decisions regarding a number of pulses and not on a pulse-to-pulse basis.

The following block diagram (Fig.1.2) visualizes the operation of the next generation Cognitive radar and presents the essential parts that compose it. The heart of the system is the processor capable of autonomous decision making. In order to make the correct decisions the processor is fed with a plethora of information and past data that will affect and eventually determine the outcome. Based on the radar's predetermined mission the characteristics of the desired targets and the initial setup of the system can be approximated according to prior knowledge from similar missions. The radar objectives nevertheless can vary over time and priorities can change constantly affecting the radar actions. In search and track applications for example, the action to be taken (i.e. search or track) is decided before

every illumination either this is based on time allocation between the modes of the radar [13] or subject to probabilistic criteria such as channel uncertainties [14].

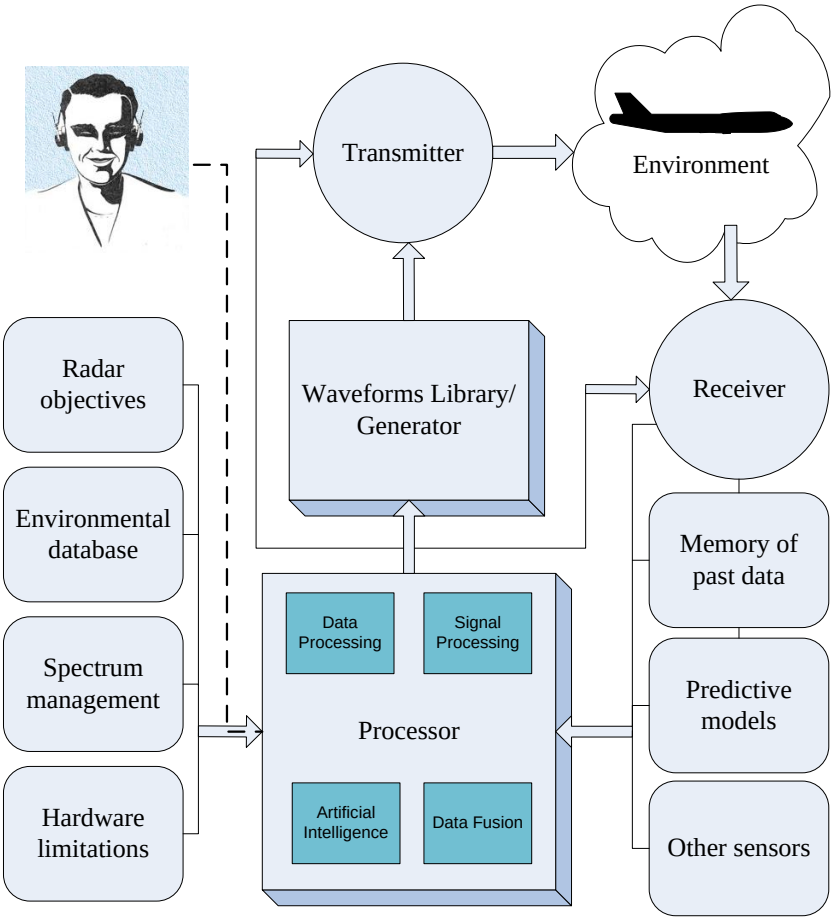

FIGURE 1.2: Block Diagram of Cognitive Radar.

A Cognitive radar that is adapting to the environment can benefit by exploiting outside data sources such as environmental databases [7] [15]. This database that includes terrain information, maps, clutter and reflectivity statistics, predicts the scattering environment and characterizes the scene to be illuminated. A dynamic environmental database including weather conditions, road traffic etc can be a continuous input to the system.

The choice of the best available spectrum for the electromagnetic emission of the radar waveforms has nowadays become an issue of great importance due to the high usage density of the spectrum. The Cognitive radar should be able to sense the electromagnetic environment [16], locate the gaps and choose the most suitable spectrum for every emission avoiding radio frequency interference and jamming [17] or develop frequency sharing techniques [18]

[19] that will limit the interference received and optimize radar performance when coexisting with overlaid wireless networks.

Implementing recent advances in the radar cycle (e.g. arbitrary waveform generators, artificial intelligence techniques, etc.) has increased the required computational power. Knowledge of the limitations imposed by hardware can help avoid system overload which would lead to potential degradation of the radar performance [20]. This will ensure the continuous and uninterrupted data flow and functionality of the system even if sometimes this will mean that information the hardware is unable to handle will be rejected or that the waveform design will be limited to the hardware capabilities. The amount of saved data such as previous measurements stored for later exploitation has to comply with the hardware limitations as well. Nonessential or older data and measurements should be replaced by new when storage is full.

Data from other sensors (e.g. images taken from sensors equipped in the radar platform that can contribute to the improved performance with their high cross-range object identification or real-time information from collaborating radars that can reduce the ambiguities of the measurements [14]) and results from predictive models based on the target behaviour, the clutter, etc. can have a beneficial impact and aid the optimization and decision process.

The received echo and data are processed, fused and artificial intelligent techniques like machine learning judge and decide the setup of the radar for the next emission. This includes the characteristics of the transmitted waveform, the beamforming, the transmit beampattern as well as the optimization of the receiver. In [14] a dynamic illumination strategy between two radars is developed based on the probabilistic representation of the environment. In every transmission the radar adjusts the beamsteering pattern according to its perception of the environment and more specifically illuminates the area with the highest channel uncertainty as calculated based on previous measurements. The beampattern design is also studied in [21] with the Cramer Rao bound (CRB) and the Reuven-Messer bound (RMB) being utilized as the criteria for optimization. In [15] the transmit signal and the receive filter are jointly designed for the improvement of the signal to interference plus noise ratio (SINR) considering the available information about noise, clutter and channel propagation.

Enhancement in the performance can also be achieved through resource allocation schemes and especially transmit power allocation. Two recent studies in multiple sensors radars [22] [23] suggest that uniform power allocation among the radar sensors is not optimal. On the contrary, an adaptive power allocation strategy can minimize the target state estimation error or reduce the total power budget.

Radars have also been used as communications systems. A method where surveillance and communication issues are addressed simultaneously from the same platform by a single waveform design has been proposed in [24].

Although the vision for the next generation radar is an entirely automatic and autonomous system, the vital contribution of the radar operator that oversights and interferes with the operation cannot be neglected until confidence in the automated process is much improved. The input from the operator is of highest priority and introduces an additional challenge to the optimization. The design of an algorithm that will be able to effectively distribute time and resources on the aforementioned aspects of the Cognitive radar cycle is one of the main challenges that need to be addressed.

All of the above information gathering and multi-function mechanisms that are under investigation reveal the tendency in the research community to integrate the radar system into a completely autonomous, intelligent and smart platform with many more capabilities than the traditional radars that will be able to scan-and-track, take pictures from high-end cameras, handle information about the environment and also communicate with other platforms exchanging data, leading to minimized ambiguities and improved performance in general.

In this thesis, motivated by the advances and recent trends in radar technology as described previously, we focus on the adaptive waveform design of the next generation radar. We demonstrate how adaptive waveform transmission is beneficial for tracking missions over the transmission of fixed waveform. The collected measurements operate as the feedback mechanism from the receiver to the transmitter and define the transmission of the next waveform. We present a method of adaptive waveform design within a sensor management problem with power limitations and finally we propose a direction towards the multi-sensor resource allocation and waveform design for further work.

1.2 Overview

In Chapter 2, the adaptive waveform design concept is introduced. First, we present the echo-location system of the bats that have motivated and are considered the physical proof of the Cognitive Radar concept. Bats interact with their environment and adapt their emitted signals accordingly. The basic hunting principle of the bats is then applied to radar through a simple scenario. The pulse repetition frequency and the bandwidth of the transmitted pulses are adapted based on the target distance from the radar. This allows us to see the benefits and trade-offs of this behaviour. Then we present the most commonly used adaptive waveform design methods and we apply the Control Theoretic Approach in a Linear Frequency Modulated (LFM) waveform for the enhancement of the tracking precision. Finally, we construct a library of adaptive waveforms (Triangular, Gaussian and Gaussian LFM) and present a collaboration strategy between two radars. The cost function used for the minimization of the tracking error chooses the parameters of the waveforms (pulse duration and chirp rate) leading to improved performance.

In Chapter 3, power considerations in the adaptive waveform design are taken into account. We are simulating a ground-based surveillance radar that can operate in either of two modes; search or track. For this reason, a sensor management technique that allocates time between the radar modes and decides the cell or target that will be illuminated in the next waveform transmission is used. The sensor management technique listens to the input by the operator about the time allocation and considers the cells' and targets' uncertainty for the choice of the illumination area. The waveform design adapts the waveform parameters for improved tracking and reduces the transmitted power when this does not affect the performance of the tracker. Then it allocates the saved power in the search mode for increased probability of detection. Overall, the transmitted power is shown to be reduced when we use this method compared to the transmission of a fixed waveform.

In Chapter 4, we extend to multi-sensor resource allocation and waveform design. The use of networks of sensors is something that becomes more and more necessary nowadays due to the huge amount of available information in the environment combined with the inability of a single sensor to efficiently gather the information or perform multiple tasks by itself. As

a consequence, the sensors have to compete for the system's limited resources such as time, bandwidth, power etc. and therefore a resource allocation technique is critical to the system performance. We propose the creation of a framework that would unify the concepts of adaptive waveform design and resource allocation in a multi-sensor system using the Cramer Rao Lower Bound (CRLB). This way we can allocate resources between the sensors of the network and at the same time design the transmitted waveform.

Conclusions to the thesis are discussed in chapter 5 where we also suggest some further work which may be a useful extension to the thesis.

Chapter 2

Adaptive Waveform Design

2.1 Introduction and Objectives

The adaptive waveform design has become one of the most crucial and inseparable components of the Cognitive Radar cycle due to the undeniable effect on the performance of the system. The objective of this chapter is to present the tools and methods that are used in the literature for adaptive waveform design purposes. We focus on the control theoretic approach and begin the adaptive waveform design analysis by formulating the problem and presenting the core of the target tracking algorithms; the recursive Bayesian estimation. Necessary tools also include the Ambiguity Function, the Cramer Rao Lower Bound and the error covariance.

We start this chapter by motivating the benefits of simple adaptive waveform approaches by simulating an echo-location system of bats. Then we build on the approaches described in the literature in the latter part of this chapter. The specific contributions are:

- An adaptive LFM waveform is presented and compared with the tracking performance of a fixed LFM waveform as well as we compare the performance of the Kalman filter against the recently proposed Cubature Kalman filter.
- We build a library of three different classes of adaptive waveforms and we highlight the increase on the tracking precision over the use of a single waveform. We also

demonstrate the benefits of collaboration between two sensors where they exchange information about their measurements but the waveforms transmitted are designed separately due to the different SNR they are experiencing.

2.2 Echo-location System of Bats

The echo-location system of the bats has motivated the next step in the evolution of dynamic radars commonly known as Cognitive Radars [9]. Every time when they move in space, search for food, or approach a target, bats continuously emit echolocation signals in order to analyse the returning echoes. These signals are ultrasonic sounds and the objects are recognized as acoustic images. The bat broadcast these signals from its mouth and uses its auditory system as a sonar receiver, where also performs the tasks of detection, localization and classification. All of these tasks are the core of the radar operations. Echo components reflected from a target have overlapping and delaying components. Bat transforms this spectrum into components of an image to find the range and shape of the target. For detection, bats must determine whether they have received echoes of their own emitted signals. For classification, bats use patterns of echo information to categorize targets. For localization, they measure the time delay between the emitted signal and the returning echo to estimate target distance. Fig.2.1 [1] shows that depending to the bat's goal, the environment and the habitat, bats performs different echolocation task. We can see the differences between the one that simply moves into space and the one that searches for prey and between different types of environment. We notice that the bat emits a long pulse in the open space whereas in the narrow space the transmitted pulses are much smaller in duration. This way the bat increases its range resolution when it moves in narrow spaces to allow for more accurate manoeuvre through the obstructions.

A Cognitive radar should embody the following three fundamental characteristics:

- Information feedback loop from the receiver to the transmitter.
- Memory of the radar returns.

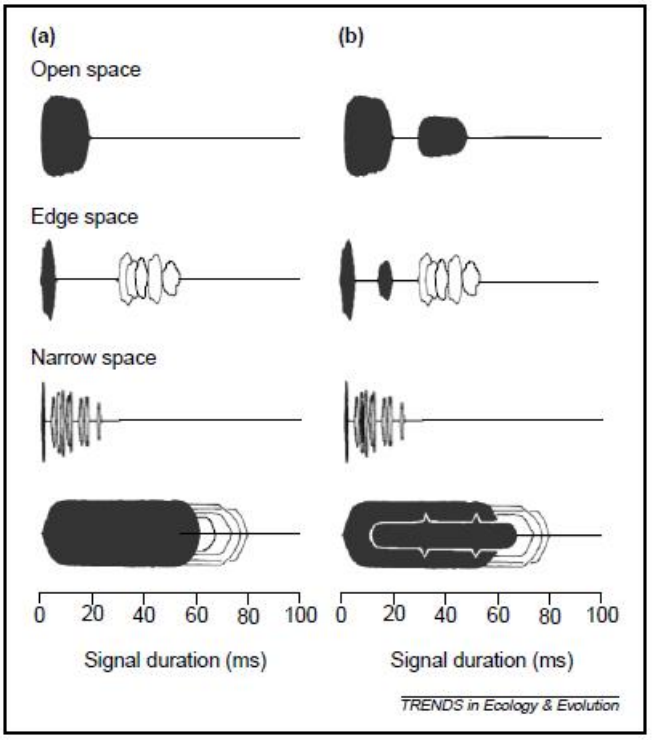

FIGURE 2.1: [1] Echolocation tasks of bats during spatial orientation (a) and search for prey (b) in different habitats. The emitted pulse and the echo returning from prey (grey) are displayed together with echo trains from background targets (white).

- Learning from the interactions with the environment.

All of these are parts of the echo-location system of the bats, which use sonar to detect the target, getting information about the target's range, velocity, elevation, azimuth and size. The success rate of the bat's target capture is so high that would be the envy of a radar engineer. Fig.2.2 [2] illustrates the spectrograms produced by four different bat species during their target pursuit.

We can see from this figure that the bat uses the acquired knowledge of the distance from the target to appropriately adjust the transmitted signal. The signal duration decreases and the burst repetition frequency increases as the bat gets closer to the target. By decreasing the signal duration the bat has increased range resolution and can estimate the position of the pray with higher accuracy whereas an increased burst repetition frequency increases the received information rate and updates faster the range estimate of the pray, a very important function as the bat gets closer and closer. This considerable change of the transmitting

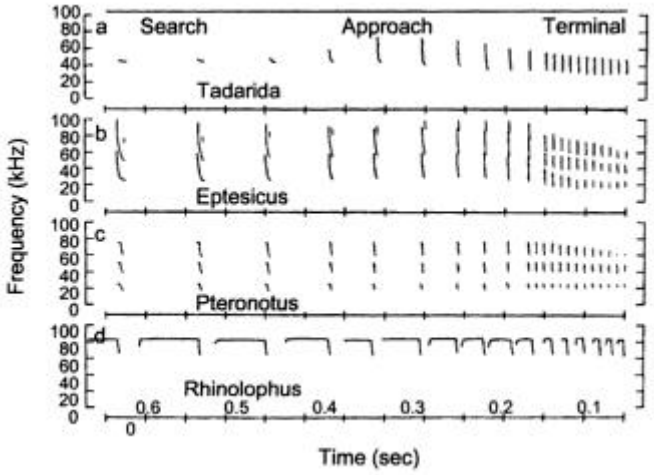

FIGURE 2.2: [2] Spectrograms of sonar signals produced by four different species of bats as they search and pursuit insects.

parameters during the different phases of the pursuit convince that the echolocation system of a bat is physical proof of cognitive radar.

The duration of the emitted waveform can vary from 0.3 to 300 ms and the frequency is from 12 to 200 kHz depending on the situation and the species. The adaptive behaviour of bats is categorised [9] in velocity adaptation, involving the frequency adjustment, and in range adaptation which is the adjustment of the signal's duration, bandwidth and repetition rate. Pulse by pulse variation of these parameters is the clue to such high accurate localization, classification, tracking and capture of the prey. When the bat's acoustic and signal processing will be understood and modelled, these techniques can be used to develop smart antennas and signal processing with immediate implementation to the Cognitive Radar concept. Then we will have a powerful and low cost tool for target localization, identification, tracking and capture or avoidance [25].

In recent researches [26] [27] [28] it is found that some species of bats emit ultrasonic biosonar sounds that contain two delayed harmonics which helps them differentiate between the objects that are located at short range and those positioned at the background. Also, some species adjust the echolocation signals (duration, bandwidth) according to the desired distance of focus, while others change the interpulse intervals according to clutter densities in order to avoid obstructions. In another research [29] it was shown that bats with different

types of pinnae (the part of the ear that resides outside of the head) had different types of beamforming mechanism through which they see the environment.

We now perform a radar simulation of a simple scenario showing the advantages of an adaptive waveform similar to the hunting principles of the bats as presented in fig.2.2. The waveform parameters that have been adapted throughout the scenario are the Bandwidth (B=1/T) and the Pulse Repetition Frequency (PRF). The scenario used for the simulations is presented in fig.2.3.

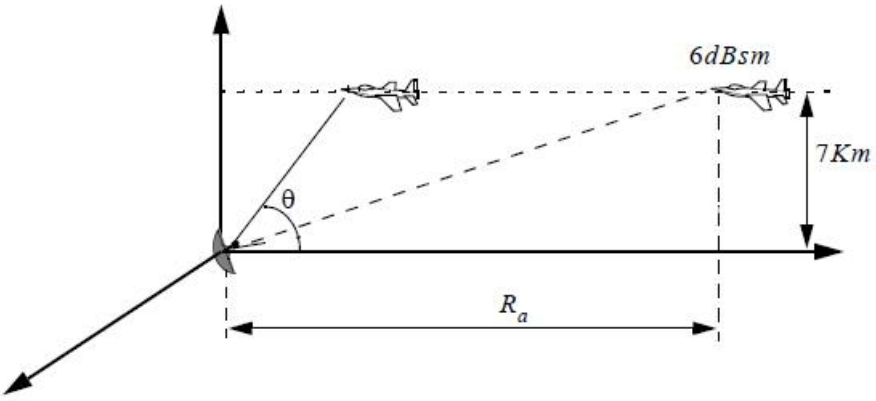

FIGURE 2.3: Radar/aircraft geometry.

A ground-based radar is simulated with objective to search and detect an aircraft with an average RCS of 6 dBsm and altitude of about 7km. It is assumed that the radar to have a scanning azimuth coverage of 360 degrees, noise figure F_n = $8dB$ and total receiver loss L_r = $10dB$. The choice of the radar operating frequency is determined by many factors (aperture size, clutter, atmospheric attenuation) which are not of our interest at the moment. In this scenario we choose f_c = $800MHz$ and antenna gain G = $22dB$. Lastly, the peak power is set to P_t = $1.2kW$. The signal used is a simple pulse described by:

$$s(t) = \frac{1}{\sqrt{T}} rect\left(\frac{t}{T}\right) \tag{2.1}$$

The first two simulations are executed keeping the pulse bandwidth constant at B_1 = $100kH$ and B_2 = $2MHz$ accordingly with PRF = $1kH$. Then the pulse bandwidth and pulse repetition frequency are linearly adapted according to the target's range. When the target is at $100km$ distance the bandwidth is set at B = $100kH$ and the pulse repetition at PRF = $1kH$

linearly increasing up to B = $2MHz$ and PRF = $15kHz$ as the target gets closer. The SNR is computed by the radar equation:

$$SNR = \frac{P_t G^2 \lambda^2 b}{(4\pi)^3 k T_e B F_n L_r r^4} \tag{2.2}$$

where k = $1.38x10^{-23} joule/degree\ Kelvin$ and T_e = $290 Kelvins$.

As expected and according to theory, the simulation results show that by increasing the pulse bandwidth we can get finer range resolution (fig.2.4). The drawback is that higher pulse bandwidth results in a lower SNR, making detection more difficult (fig.2.5). This trade-off between SNR and range resolution determines the choice of the pulse bandwidth. As the target gets closer the need for better range resolution increases while at the same time the SNR has reached a certain level that will make the detection feasible and will allows us to increase the pulse bandwidth. The connection between the pulse repetition frequency (PRF) and maximum unambiguous range is presented in fig.2.6. In order to have a maximum unambiguous range of 150km we use PRF of 1 kHz which is sufficient when the target is 100km away. As the target gets closer we increase the PRF in a way that will constantly keep the maximum unambiguous range higher than the actual target range.

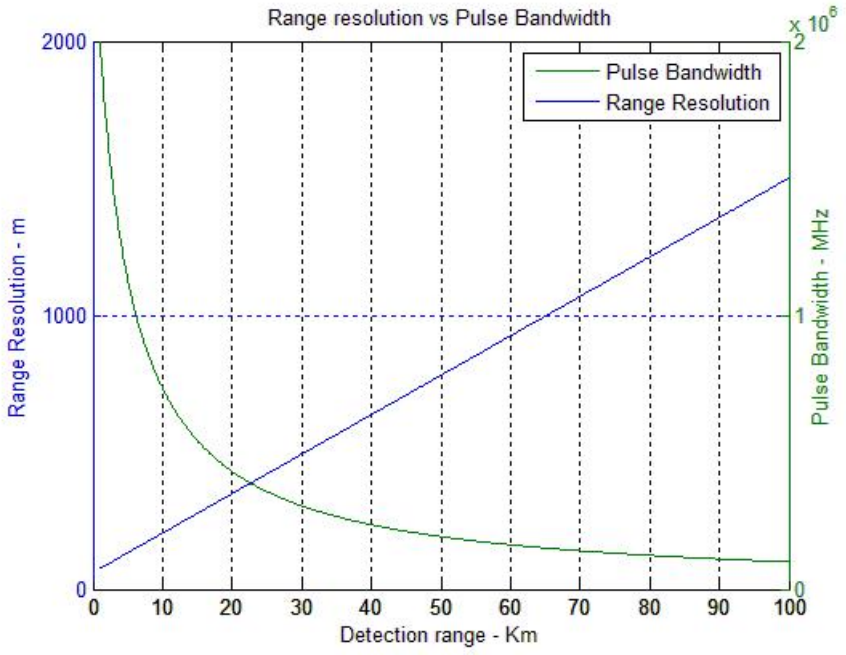

FIGURE 2.4: Range resolution vs Pulse Bandwidth.

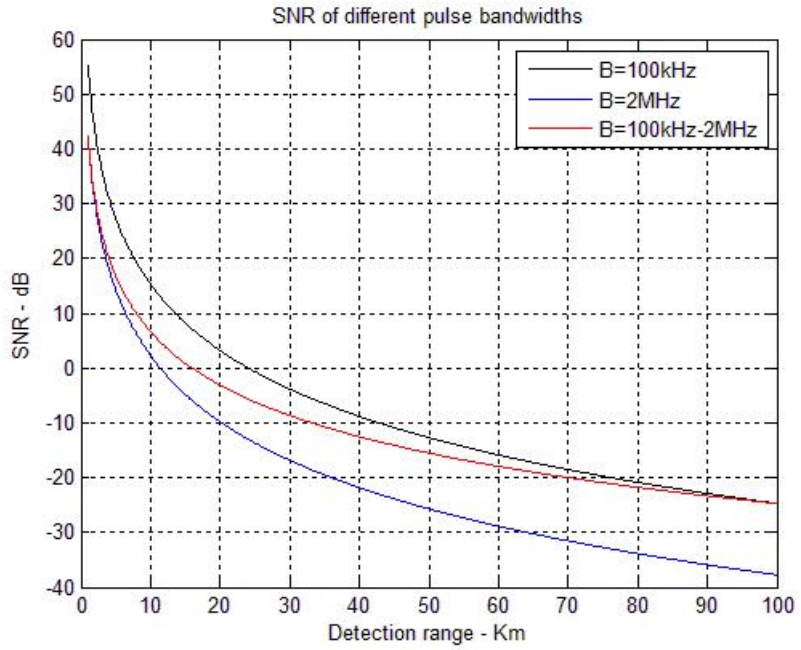

FIGURE 2.5: SNR of different pulse bandwidth.

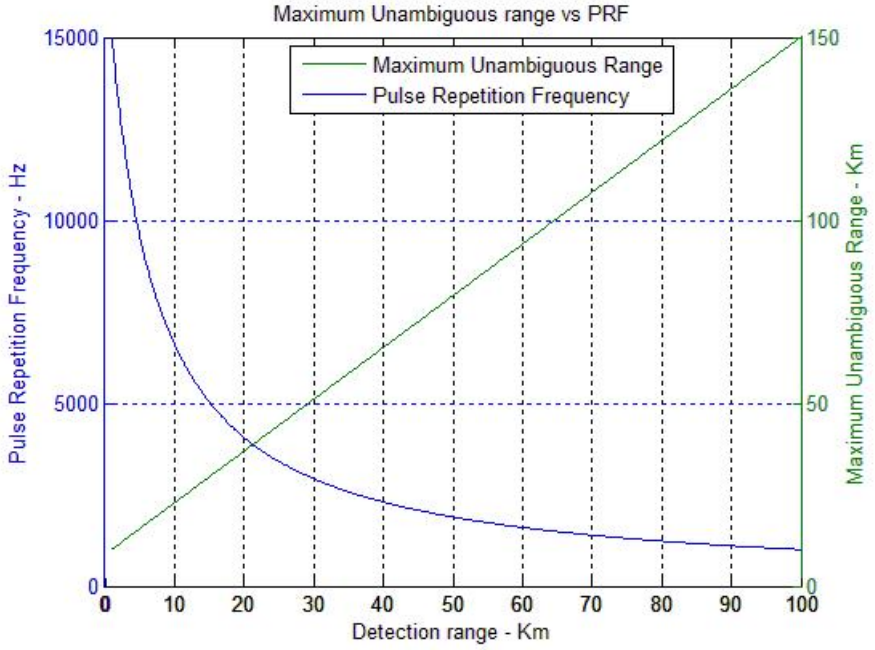

FIGURE 2.6: Maximum Unambiguous Range vs PRF.

2.3 Waveform Design Literature Review

The adaptive waveform design concept can be described as the process where the design of the next transmitted waveform is optimized to improve the performance and comply with the radar objectives. The effect of waveform adaptivity in the performance of the radar has indisputably made adaptive waveform design a crucial component of the Cognitive Radar cycle. Changes in the dynamic environment of the radar such as signal-to-noise ratio (SNR), clutter and target state directly affect the performance of the system. Adaptive waveform design exploits the above information and adjusts the parameters of the next transmitted waveform or set of waveforms (e.g. the pulse width or/and the chirp rate etc.) accordingly to match the dynamic environment and the mission of the radar. The flexibility provided to the system to choose or create the desired waveform results in improved performance metrics such as target tracking, detection, target recognition, interference avoidance etc. Increased sensor capabilities, waveform generators and real time signal processing are some of the latest advances in technology that are utilized.

Several approaches and tools (Fig.2.7) have been used for adaptive waveform design in radar with most of them being application-dependant. This means that the waveform design has a very specific objective and in most cases is focusing on the enhancement of one performance metric at a time. The development of an adaptive waveform design technique that will tackle the multiple performance measures (e.g. target detection and tracking, target recognition, power save, interference avoidance) under a single unified framework is the next step towards a powerful next generation dynamic radar. A review of the latest and most commonly used adaptive waveform approaches and their application is presented in this chapter, focusing on the control theoretic approach which will be the main method for the rest of the thesis due to its close link with tracking applications.

The aid of an automatic tool due to the high number of performance and technical details to consider for waveform design is highlighted in [30]. A three step algorithm that selects the best waveform that fits the requests is presented. First the waveform parameters such as carrier frequency and chirp code are selected by the operator or other functions, then the PRF is determined according to the clutter scenario and finally the choice of the dwell time

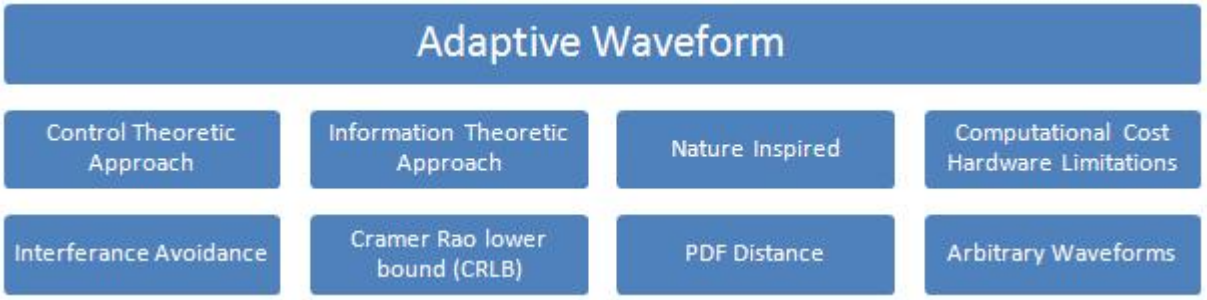

FIGURE 2.7: The variety of approaches and tools used in adaptive waveform design.

needed to guarantee the requested signal-to-noise ratio is made. In [31], the joint use of stepped frequency chirps, Costas codes and pushing sequences [32] is proposed to form an effective signal for adaptive waveform radar. All of them are easily generated and processed using common hardware and combining the different characteristics of these waveforms we can get enhancement of the delay-Doppler resolution. For example, the author in [31] suggests using chirp waveforms for detection, Costas codes to resolve targets and finally pushing sequences to ensure that there are no small scatterers close to the mainlobe response.

2.3.1 Nature Inspired

The idea of Cognitive Radar was first inspired by the echo-location system of the bats and is therefore expected that waveform design techniques inspired by nature are studied. It is found that some species of bats emit ultrasonic biosonar sounds that contain two delayed harmonics which helps them differentiate between the objects that are located at short range and those positioned at the background. Multi-harmonic waveforms are studied in [33] and results show that they can improve range resolution, reduce sidelobes and offer another degree of freedom in waveform design. The tracking performance of manoeuvring targets is studied in [34], inspired by the adaptive behaviour of bats. The radar is mounted on a moving platform and both waveform and trajectory design is proposed. The proposed method shows that the model with low acceleration variance can accurately estimate targets with constant velocity but fails to track manoeuvring targets, while a high acceleration variance model keeps track of manoeuvring targets but has a higher estimation error, therefore the high acceleration model is assigned with a low PRI (pulse repetition interval). When a manoeuvre

is detected the PRI is decreased and when the target moves in a straight trajectory the PRI is increased resulting to lower computation load and power consumption.

2.3.2 Arbitrary Waveform Design

Arbitrary waveform design has become feasible with the evolution of waveform generators where both the modulus and the phase of the waveform can be designed. Arbitrary waveform design has attracted the interest of researchers and has been utilized in a variety of applications but the drawback of this approach is the increased computational complexity it requires. The objective of [20] is to design a waveform that will maximize the signal to interference plus noise ratio (SINR) taking into account real world system constraints and hardware limitations. As noted, the potential for the system performance increases with the increase of the degrees of freedom. Most of them are offered in the arbitrary waveform design, that almost no structure is assumed, and recent advances in technology have made them a practical possibility. On the other hand, constraints imposed by digital-to-analogue converters (part of the transmit system) and power amplifiers (i.e. peak power, constant modulus) if are not incorporated in the waveform design algorithm can cause degradation of the system performance. Also keeping in mind the need to constrain the autocorrelation sequence (ACS) of the transmit waveform to retain specific waveform characteristics, the author concludes to the following optimization problem for arbitrary waveform design:

$$\begin{aligned} & \max s^H R_i^{-1} s \\ \text{Subject to}: \quad & |s(n)| \leq M_{in}, \qquad n = 1, 2, \dots N \\ & \left|s^H U^k s\right|^2 \leq m(k), \; k = 0, \dots N-1 \end{aligned} \tag{2.3}$$

where H denotes conjugate-transpose, s is the transmit signal vector, R_i is the interference-plus-noise covariance matrix, M_{in} is the maximum input modulus, U is a upper shift matrix and $m(k)$ is the maximum allowable squared-magnitude. Results in [20] show that neglect of modulus constraints can give rise to serious performance degradation. Similar approach for the maximization of the SINR is followed in [15]. Limitations on the transmitted energy and the desired ambiguity function behaviour equivalent to the constrains in [20] are set.

The studies in [17] and [18] deal with the problem of interference avoidance when the radar operates in a spectral dense environment. The adjacent-band and the in-band interference are considered in [17]. The main idea is that in battlefield scenarios, on the one hand you want to avoid friendly interference by other RF transmitting devices that may occupy similar frequency bands and at the same time you want to avoid hostile jamming, excluding frequencies that match any in-band interference. An adaptive waveform technique is presented that covers the above points while maintaining good ambiguity function performance. The waveforms used are LFM because of their attractive properties such as high range resolution, constant modulus, Doppler tolerance and implementation simplicity. Assuming that the interference can be estimated by measurements of transmit-free or 'listen only' samples, spectrum estimation can be formed and the appropriate template is selected. The adaptive LFM waveform is formulated as the least squares weight vector:

$$s_0 = \frac{R^{-1}(s)}{s^H R^{-1}(s)} \tag{2.4}$$

where s_0 is the adaptive waveform vector and R is the interference covariance matrix. This method constructs a waveform that remains similar to the LFM but attenuates interference spectra components but comes to the cost of a modest loss of Doppler tolerance. In [18] the waveform design aims to maximize the probability of detection by improving the SINR when operating in spectral coexistence. It is shown that a trade-off between the desired characteristics of the waveform and enhanced interference avoidance takes place.

2.3.3 Probability Density Function Distance

A waveform design technique for target recognition based on the maximization of the distance between the probability density functions has been proposed in [35]. In the case of 2 possible targets the target autocorrelation matrix at time step k is described by $\Omega_k = (Q_1 - Q_2)^T(Q_1 - Q_2)$ where Q_1 and Q_2 represent the target convolution matrix of the first and second target respectively and $(\cdot)^T$ the transpose. The optimum waveform vector s_k is the one that maximizes the Euclidean distance between the mean values of the two probability density functions and is the vector that maximizes $s_k^T \Omega_k s_k$. While this method in

[35] suggests arbitrary waveform design, in [36] the same technique is used for single-tone waveforms with constant envelope. The performance of the single frequency waveform is almost similar to the arbitrary waveform with highly reducing the computational cost.

2.3.4 Information Theoretic Approach

An important adaptive waveform design technique is the Information Theoretic Approach which is based on the concept of the mutual information. The mutual information between the target and the measurements is a method to express the amount of information the measurements are providing about the target denoted by $\mathbf{I}(X_k, Y_k)$, where X_k denotes the target state and Y_k the radar measurements in time step k respectively. In this context the goal is to maximize the mutual information between the target and the measurements leading to more accurate estimation of the target state. The expected mutual information when utilizing Kalman filter is given by [37]:

$$\mathbf{I}(X_k, Y_k) = \log\left(\det\left(I + R(\theta_k)^{-1} P_{k|k}\right)\right) \tag{2.5}$$

where θ_k denotes the waveform parameters at time step k, $R(\theta_k)$ the covariance of the measurement noise and $P_{k|k}$ the covariance of the state estimation (R, $P_{k|k}$ are defined in Chapter 2.3.5). The criterion in this case is to select the waveform with parameters θ_k from the set of the available waveform parameters Θ that will maximize the mutual information $\mathbf{I}(X_k, Y_k)$ according to:

$$\theta^*_{k+1} = \underset{\theta_{k+1} \epsilon \Theta}{\arg\max}\, \mathbf{I}(X_k, Y_k) \tag{2.6}$$

A two-step algorithm for adaptive waveform design using this approach is proposed in [38]. The first step designs the transmission signal ensuring that the received echoes will be statistically dependant on the target features, maximizing the mutual information between the received echo and the target response. The second step selects the waveforms making sure that the acquired echoes are more statistically independent on each other, minimizing the mutual information between successive received signals in order to gain more knowledge for the target features at each time. In other words, successive target echoes are as different

from each other as possible. Similar technique for maximizing the mutual information is also used in [39] for target recognition purposes.

A technique for estimating the mutual information based on a quantity known as spectral variance leading to direct design of the transmitted waveform was proposed in [40]. According to this study the waveform that maximizes the mutual information has the magnitude-squared spectrum defined by:

$$|S_k(f)|^2 = max\left[0, A_k - \frac{R_k(f)T_y}{2\sigma_H^2(f)}\right] \tag{2.7}$$

where T_y is the interval during which the received signal is observed, σ_H^2 is the spectral variance and A_k is obtained by constraining the total energy of the transmitted waveform. This approach is used in [41] [42] and the authors concluded that for detection the optimal radar waveform should put as much energy as possible to the largest scattering mode of the target to maximize SNR while for estimation the optimal radar waveform should distribute the energy among the target's scattering modes in order to maximize the mutual information. The technique proposed in [42] minimizes the Bayesian CRB of the unknown parameter where each waveform of the pulse train is adaptively designed based on the previously received data. Simulations at low SNR level result to higher rate of reduction of the root mean square error (MSE) compared to identical waveform transmissions.

An alternative on the mutual information-based design is given in [43] based on the concept of free energy. The research states that minimizing the free energy that is dependent of the radar target return leads to the same performance as the mutual information method and can at the same time be used for the estimation of a single parameter similarly to the MSE method.

2.3.5 Control Theoretic Approach

The control theoretic approach is the main adaptive waveform design technique used in this thesis and before further analysis it is important to present the recursive Bayesian estimation for the target-tracking problem. The models for the target dynamic X_k and the noisy measurements Y_k are needed for the estimation of the target state parameters at time

step k like position, velocity and acceleration denoted by $\hat{X}_k$. A discrete-time dynamic system is generally described by the following state and measurement equations:

$$X_k = f(X_{k-1}) + W_{k-1} \tag{2.8}$$

$$Y_k = h(X_k) + V_k \tag{2.9}$$

where W is the process noise vector with covariance matrix Q, $W \sim N(0, Q)$, Y is the measurement vector and V is the measurement noise vector with covariance matrix R, $V \sim N(0, R)$. f is the transition function that described the motion of the target and h is the transformation function that describes how the measurements Y_k are related to the to the target state X_k and are generally non-linear. In linear cases the transition function f is described by the transition matrix F and similarly the transformation function h by the transformation matrix H. The objective of the tracker is to estimate the target state X_k based on the previous measurements $Y_1 \dots Y_k$. The tracker estimates the probability density function (pdf) $p(X_k \mid [Y_1 \dots Y_k])$ where the mean of the pdf is the estimation of the target state.

In the recursive Bayesian estimation context the prediction step is performed using the Chapman-Kolmogorov equation:

$$p(X_k \mid [Y_1 \dots Y_{k-1}]) = \int p(X_k \mid X_{k-1})\, p(X_{k-1} \mid [Y_1 \dots Y_{k-1}])\, \mathrm{d}X_{k-1} \tag{2.10}$$

with $p(X_k \mid X_{k-1})$ usually described by the Markov transition using the motion model of the target $f(X_{k-1})$ and $p(X_{k-1} \mid [Y_1 \dots Y_{k-1}])$ is the posterior density at time step $k-1$. In the next step the received measurements Y_k update the predictive density $p(X_k \mid [Y_1 \dots Y_{k-1}])$ according to Bayes' rule:

$$p(X_k \mid [Y_1 \dots Y_k]) = \frac{p(Y_k \mid X_k)\, p(X_k \mid [Y_1 \dots Y_{k-1}])}{p(Y_k \mid [Y_1 \dots Y_{k-1}])} \tag{2.11}$$

where $p(Y_k \mid X_k) = N(Y_k, h(X_k), R)$ and
$p(Y_k \mid [Y_1 \dots Y_{k-1}]) = \int p(Y_k \mid X_k)\, p(X_k \mid [Y_1 \dots Y_{k-1}])\, \mathrm{d}X_k$ is a normalizing constant which doesn't have to be calculated when we employ Kalman filter. Finally the updated

posterior density takes the form:

$$p\left(X_k \mid [Y_1 \dots Y_k]\right) \propto p\left(Y_k \mid X_k\right) p\left(X_k \mid [Y_1 \dots Y_{k-1}]\right) \tag{2.12}$$

Based on the characteristics of the models used to describe the target motion and the measurements the appropriate tracking algorithm should be chosen. When functions f,h are linear, Kalman filter is the obvious choice achieving the highest accuracy while minimizing the computational cost. In this case the mean denoted by $\hat{X}_{k|k-1}$ and the covariance denoted by $P_{k|k-1}$ of Eq.(2.10) are calculated by:

$$\hat{X}_{k|k-1} = F_{k-1}\hat{X}_{k-1} \tag{2.13}$$

$$P_{k|k-1} = F_{k-1}P_{k-1}F_{k-1}^T + Q_{k-1} \tag{2.14}$$

with F_{k-1} representing the transition matrix at time step $k-1$, $\hat{X}_{k-1}$ the mean and P_{k-1} the covariance of the posterior density at time step $k-1$ and Q_{k-1} the covariance of the process noise at time step $k-1$. T denotes the conjugate.

The mean and covariance of Eq.(2.12) denoted by $\hat{X}_{k|k}$ and $P_{k|k}$ respectively are calculated by the Kalman filter according to:

$$\hat{X}_{k|k} = \hat{X}_{k|k-1} + K_k\left(Y_k - H_k\hat{X}_{k|k-1}\right) \tag{2.15}$$

$$P_{k|k} = \left(I - K_kH_k\right)P_{k|k-1} \tag{2.16}$$

where H_k denotes the transformation matrix at time step k,I is the identity matrix and K_k the Kalman gain described by:

$$K_k = P_{k|k-1}H_k^T\left[H_kP_{k|k-1}H_k^T + R(\theta_k)\right]^{-1} \tag{2.17}$$

R_k represents the covariance of the measurement noise at time step k. Eq.(2.13) - Eq.(2.17) form the Kalman filter. The mean of the updated posterior density $\hat{X}_{k|k}$ is considered to be the estimated state of the target and $P_{k|k}$ the covariance of the estimation.

Introducing the adaptive waveform design concept, the tracker will select the desired waveform from a waveform library or generator according to the chosen cost function. The waveform affects the next measurements and therefore the estimation of the pdf will also depend on the waveform parameters selected denoted by the vector θ_k, $p\left(X_k \mid [Y_1 \dots Y_k], [\theta_1 \dots \theta_k]\right)$. θ_k can contain the pulse duration, the sweep rate of an FM waveform, the peak power, etc. depending on the transmitted waveform. When the posterior density P_{k-1} is non-Gaussian or the state and observation models are non-linear the conditions for the Kalman filter are no longer valid. In these scenarios we need to employ other estimation techniques such as non-linear alterations of Kalman filter or Particle filter.

A very important element of the waveform design for the control theoretic approach is the process that predicts the expected observation error. The ambiguity function (AF) (as presented in more details in Appendix B) of the received waveform is a two-dimensional function of time delay and Doppler frequency showing the distortion of the returned pulse [44]. It is used to determine the range and Doppler resolution for a specific radar waveform and gives the accuracy on the estimation of delay and Doppler of the targets. Assuming high SNR the sidelobes of the AF are low and can be neglected. Then the sensor can be assumed to achieve the Cramer Rao Lower Bound (CRLB) on the measurement error covariance R [11]. The CRLB can be calculated directly from the second derivative at the origin of the AF and the measurement error covariance matrix R is then described by:

$$R = \mathbf{E}[(Y - \bar{Y})(Y - \bar{Y})^T] = B_r J^{-1} B_r^T \tag{2.18}$$

where T denotes the conjugate, $\mathbf{E}[\cdot]$ the expected value, $\bar{Y}$ the mean of measurements Y, J the Fisher matrix of the CRLB. B_r is the transformation matrix between the received parameter vector of time delay τ and Doppler frequency ω and the tracking system measurement vector of range r and velocity v, $r = c\tau/2$ and $v = c\omega/2f_c$.

$$B_r = \mathrm{diag}\left(\frac{c}{2}, \frac{c}{2f_c}\right) \tag{2.19}$$

with f_c representing the carrier frequency. The fisher matrix is calculated according to the equation:

$$J_{ij} = -n\frac{\partial^2 \chi(A)}{\partial A_i \partial A_j} \tag{2.20}$$

where n is the SNR, $A = [\tau, \omega]$and J_{ij} is the two dimensional matrix:

$$J_{ij} = \begin{bmatrix} J_{11} & J_{12} \\ J_{21} & J_{22} \end{bmatrix} \tag{2.21}$$

with

$$\begin{aligned} J_{11} &= -n\frac{\partial^2 \chi(\tau,\omega)}{\partial \tau^2} \\ J_{12} = J_{21} &= -n\frac{\partial^2 \chi(\tau,\omega)}{\partial \tau \partial \omega} \\ J_{22} &= -n\frac{\partial^2 \chi(\tau,\omega)}{\partial \omega^2} \end{aligned} \tag{2.22}$$

Looking at Eq.(2.18) - Eq.(2.22) we notice that the measurement error covariance matrix R depends only on the waveform's characteristics and therefore is affected by the choice of the parameters of the waveform denoted by the vector θ_k. Eq.(2.18) can be written as:

$$R(\theta_k) = B_r J(\theta_k)^{-1} B_r^T \tag{2.23}$$

Assuming that the target state is sufficiently described by the mean and the covariance of the corresponding probability density function we can choose a criterion that will adjust the waveform's parameters leading to the minimization of the tracking mean-square error (MSE) which is given by the trace of the expected state covariance. The criterion for the selection of the appropriate waveform parameters vector θ_k according to the problem statement as analysed previously in this section will be:

$$\theta_{k+1}^* = \underset{\theta_{k+1} \in \Theta}{\arg\min}\, Tr\left\{Cov[p(X_k \mid [Y_1 \dots Y_k], [\theta_1 \dots \theta_k])]\right\} \tag{2.24}$$

with Θ denotes the set of the available waveform parameter vector.

As discussed previously, when using Kalman filters the expected state covariance matrix $P_{k|k}$ of the updated posterior density $p\left(X_k \mid [Y_1 \dots Y_k], [\theta_1 \dots \theta_k]\right)$ is iteratively calculated by:

$$P_{k|k} = P_{k|k-1} - P_{k|k-1} H_k^T \left[H_k P_{k|k-1} H_k^T + R(\theta_k) \right]^{-1} H_k P_{k|k-1} \tag{2.25}$$

where $P_{k|k-1}$ is the predicted covariance matrix at time k and H is the observation matrix and θ_k the vector containing the adaptive parameters of the waveform. The cost function can be written as:

$$\theta_{k+1}^* = \underset{\theta_{k+1} \epsilon \Theta}{\arg\min}\, Tr\left\{ P_{k+1|k+1}(\theta_{k+1}) \right\} \tag{2.26}$$

Having predetermined discrete values for the available waveform parameters described by Θ, Eq.(2.26) is calculated for every set of the available parameters and the combination that gives the lowest value is chosen for the next transmission in every time step k.

LFM waveforms with adaptive pulse duration and bandwidth have been used in [45] and [46]. The waveform used in [45] is $s(t) = \sqrt{2} Re\left\{ \sqrt{E_T} \tilde{s}(t) exp\left[2\pi f_c t\right] \right\}$, where E_T is the signal's energy and $\tilde{s}(t)$ is the complex envelop described by: $\tilde{s}(t) = \left(\pi T^2\right)^{-1/4} exp\left[-\left(\frac{1}{2T^2} - j\mu \right) t^2 \right]$ with μ representing the chirp rate. The vector $\theta = [T, \mu]$ denotes the two waveform parameter that is optimized. The dynamic waveform selection on the transmitter responds to feedback from the receiver who has a Bayesian filter where the algorithm selects the parameters θ_k minimizing the tracking error according to $\theta_k = \arg\max_{\theta_k \epsilon \Theta_k} E_{z_k, x_k | I_k, \Theta_k} \{ g(\Theta_k, I_k) \}$, where g is the cost function: $g(\Theta_k, I_k) \approx Tr\left[\Lambda P_{k|k} \right]$, P is the expected update state and Λ is a weighting matrix. In [47] the minimization of the CRLB is performed to obtain the optimal weights on each subcarrier of the OFDM signal where multipath reflections and information beyond the LOS radar returns are exploited by the authors. In [48] the carrier frequencies of the pulses are adaptively designed according to the observed scene for the reduction of the estimation errors and in [49] the selection of the appropriate pulse repetition interval (PRI) that minimizes the tracking error is studied based on the control theoretic approach. The problem of detecting low radar cross section (RCS) targets on the surface of the sea is analysed in [50]. Low grazing angles and high sea states result to low signal-to-clutter ratio (SCR) making particularly challenging the detection of small targets. Utilizing the control theoretic approach and incorporating clutter statistics into the design of a waveform can improve the signal to clutter ratio and the detection performance. The design of the

phase modulated waveform in this study is made such that its autocorrelation function takes values close to zero at those points that the clutter is estimated to have the highest energy. Minimizing the trace of the expected state covariance matrix is also addressed in [51] where two kind of problems are formulated: minimizing the sum MSE (Min-Sum-MSE) and minimizing the maximum MSE (Min-Max-MSE). Each problem is divided into two sub-problems: first the optimal observation matrix is estimated and then the parameters that are closer to this observation matrix are calculated under a constraint. The two step algorithm causes a minimal performance loss but the tracking performance is close to the one of the unconstraint problem.

2.4 Adaptive LFM Waveform

In this section, an adaptive Linear Frequency Modulated waveform and Kalman filter is used in order to present the improvement on the tracking precision of an adaptive waveform compared to the transmission of a fixed waveform. X_k represents the state vector and Y_k the observation vector of the target as described by:

$$X_k = F_{k-1}X_{k-1} + W_{k-1} \tag{2.27}$$

$$Y_k = H_kX_k + V_k \tag{2.28}$$

where $X = [r, v]$ with r representing the range and v the velocity of the target, F_k is the transition matrix, H_k is the observation matrix, W_k is the stationary white process noise with covariance matrix Q_k, $W_k \sim N(0, Q_k)$ and V_k is the stationary white observation noise with covariance matrix R_k, $V_k \sim N(0, R_k)$. The algorithm of the filter is described by Eq.(2.13)-Eq.(2.17). The LFM signal is formulated as:

$$s(t) = \frac{1}{\sqrt{T}}\text{rect}\left(\frac{t}{T}\right)\exp\left[j2\pi\left(f_ct + \frac{1}{2}\mu t^2\right)\right] \tag{2.29}$$

where T is the pulse duration and μ the sweep rate. Adjusting the bandwidth $B = \mu T$ and the pulse width T of the waveform, the covariance matrix R_k is then influenced as explained by Eq.(2.18)-Eq.(2.23). Based on the control theoretic approach the waveform is adapted

according to the cost function in Eq.(2.26) which is rewritten here:

$$\theta^*_{k+1} = \arg\min_{\theta_{k+1}\epsilon\Theta} Tr\left\{P_{k+1|k+1}(\theta_{k+1})\right\} \tag{2.30}$$

with parameter vector $\theta = [B, T]$.

By choosing the appropriate combination of bandwidth B and pulse width T the mean square error can be minimized leading to the optimized solution for the target tracking algorithm. The model that was used is a constant velocity model with target speed 100m/s and initial range 0m. The transition matrix $F = [1\ t; 0\ 1]$, the observation matrix $H = [1\ 0; 0\ 1]$ and the covariance matrix $Q = 0.001 * [1/4\ 1/3\ 1/2\ 1]$. The SNR is set to $n = 5$, the pulse width T is adjusted from 0.1ms to 1ms and the bandwidth B from 1 KHz to 10 KHz. The mean square error was estimated after 200 Monte Carlo simulations with 300 sample points. The fixed waveform was set to $T = 0.6ms$ and $B = 3KHz$. Fig.2.8 shows the result of the simulation where we can clearly notice the improvement on the tracking precision.

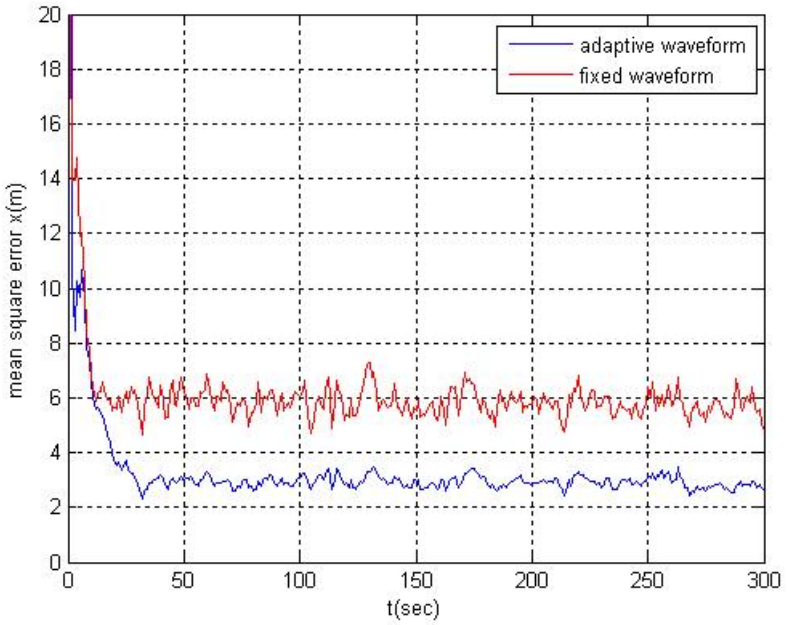

FIGURE 2.8: Mean square error of fixed and adaptive waveforms.

2.4.1 Overview of Tracking Algorithms

The literature review on adaptive waveforms reveals that an important part of the adaptation process is the target tracking method. It is therefore important to provide a short description of the main tracking algorithms that we could choose for our simulation and highlight the differences between. Kalman filter is extensively used along with the Extended Kalman filter, the Cubature Kalman filter [52], the Particle filter and the Interacting Multiple Model.

- Kalman filter (KF) is the base on which a lot of the tracking algorithms are designed. Kalman filter is an optimum solution to the least squares problem, meaning that the square error is minimized. It is a serial algorithm because it is only dependent from the current state measurement estimation and the relative covariance of the measurement and covariance of the estimation matrices. Kalman filter does not demand a lot of computational power, but is not designed to track manoeuvring or multiple targets and cannot handle clutter. Although it can be adjusted to track manoeuvring targets, the solution is not optimum.

- The Extended Kalman filter (EKF) is used in scenarios where the mapping of the coordinates is not linear. EKF is also used in situations where the measurement procedure or the dynamic of the targets are not linear. According to [53] when the starting conditions are unclear, the non-linear transformation results in a biased solution, the calculation of the covariance is not precise and the EKF can diverse.

- Interacting Multiple Model (IMM) tracking is used to predict the current state of the target using two or more different models of the target's movement. For instance, if the target is expected to be a manoeuvring target the models used could be a straight line model, a left turn model and a right turn model. Other models can be elevation or acceleration models, depending on the scenario studied.

- Cubature Kalman filter (CKF) is a relatively new nonlinear filter for state estimation in high-dimensions. CKF is computationally more expensive compared to the EKF but it can perform better in problems with more severe nonlinearities in a Gaussian environment.

- The Particle filter is usually used as an alternative of the EKF achieving more accurate estimations when the samples are sufficient but it can suffer from high-dimensionality problems leading to poor performance. It can model any probability distribution either it is continuous or discrete and has the ability to deal with non-Gaussian noise as well. It can include multiple models for tracking manoeuvring targets but its computational complexity is high.

The choice of the appropriate algorithm depends on the nature of the scenario and the trade-off between accuracy and complexity. A comparison between the Kalman filter and the Cubature Kalman filter in adaptive waveform for the above scenario is presented below. This is the algorithm of the Cubature Kalman filter as described in [54] where the dimensions of the measurement vector is denoted by n and i denotes the ith column of the matrix:

Generate sigma points and weights (w) associated with them:

$$X_{i_{k|k}} = X_0 + \left(\sqrt{P_{k|k}}\right)_i \ , \ i \leq n \tag{2.31}$$

$$X_{i_{k|k}} = X_0 - \left(\sqrt{P_{k|k}}\right)_i \ , \ n \leq i < 2n \tag{2.32}$$

$$w_i = 1/2n \ , \ i \leq 2n \tag{2.33}$$

Mean and covariance of the predicted state:

$$X_{i_{k+1|k}} = F_k X_{i_{k|k}} \tag{2.34}$$

$$\hat{X}_{k+1|k} = \sum w_i X_{i_{k+1|k}} \tag{2.35}$$

$$P_{k+1|k} = Q_k + \sum w_i \left[X_{i_{k+1|k}} - \hat{X}_{k+1|k}\right]\left[X_{i_{k+1|k}} - \hat{X}_{k+1|k}\right]^T \tag{2.36}$$

Measurement prediction:

$$Y_{i_{k+1|k}} = H_k X_{i_{k+1|k}} \tag{2.37}$$

$$\hat{Y}_{k+1|k} = \sum w_i Y_{i_{k+1|k}} \tag{2.38}$$

Innovation covariance matrix and filter gain:

$$S_{k+1|k} = R_{k+1} + \sum w_i \left[Y_{i_{k+1|k}} - \hat{Y}_{k+1|k} \right] \left[Y_{i_{k+1|k}} - \hat{Y}_{k+1|k} \right]^T \tag{2.39}$$

$$W_{k+1|k} = \sum w_i \left[X_{i_{k+1|k}} - \hat{X}_{k+1|k} \right] \left[Y_{i_{k+1|k}} - \hat{Y}_{k+1|k} \right]^T \tag{2.40}$$

Update state and covariance:

$$\hat{X}_{k+1|k+1} = \hat{X}_{k+1|k} + W_{k+1|k} \left[Y_{k+1} - \hat{Y}_{k+1|k} \right] \tag{2.41}$$

$$P_{k+1|k+1} = P_{k+1|k} - W_{k+1} S_{k+1} W_{k+1}^T \tag{2.42}$$

Fig.2.9 depicts the results of the simulation. It is clear that the Kalman filter outperform the Cubature Kalman filter. The reason is that the specific scenario matches better with the Kalman filter than the Cubature Kalman filter. It is a linear constant velocity scenario without any manoeuvre of the target which gives advantage to the Kalman filter whereas the Cubature filter is working under approximations. In complex and nonlinear scenarios the Cubature Kalman filter, even though it is more computationally complex, is expected to achieve better tracking precision.

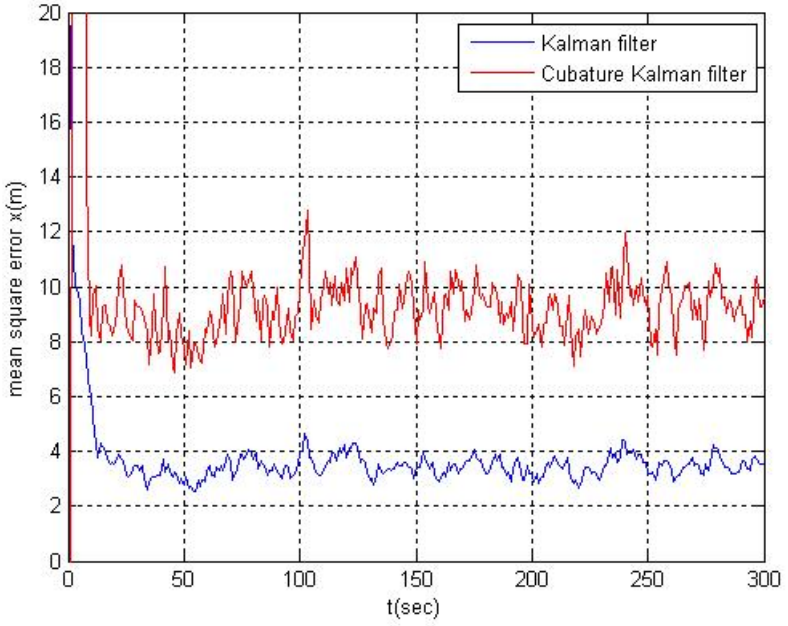

FIGURE 2.9: Mean square error of Kalman Vs Cubature Kalman filters.

2.5 Library of Adaptive Waveforms and Collaboration Strategy

In this simulation we consider the adaptive design of the transmitted waveforms which includes the choice of the waveform class (Triangular, Gaussian, Gaussian LFM) and the selection of the pulse duration and bandwidth aiming to decrease the mean square error of the response estimation based on the target impulse response and its dynamic model. The control theoretic approach is adopted and we build a waveform library consisting of Triangular CW pulses, Gaussian CW pulses and Gaussian LFM pulses with complex envelop and measurement noise covariance matrix R that are described by [11]: Triangular CW pulse:

$$\tilde{s}(t) = \begin{cases} \sqrt{\frac{3}{2T}}\left(1 - \frac{|t|}{T}\right) & \text{when } -T < t < T \\ 0 & \text{otherwise} \end{cases} \tag{2.43}$$

$$R(\theta_k) = \begin{bmatrix} \frac{c^2T^2}{12n} & 0 \\ 0 & \frac{5c^2}{2(2\pi f_c)^2T^2n} \end{bmatrix} \tag{2.44}$$

θ_k denotes the waveform parameters vector that is adjusted which for the Triangular CW pulse is $\theta_k = T$, with T representing the pulse duration. Gaussian CW pulse :

$$\tilde{s}(t) = \left(\frac{1}{\pi T^2}\right)^{1/4} \exp\left(\frac{-t^2}{2T^2}\right) \tag{2.45}$$

$$R(\theta_k) = \begin{bmatrix} \frac{c^2T^2}{2n} & 0 \\ 0 & \frac{c^2}{2(2\pi f_c)^2T^2n} \end{bmatrix} \tag{2.46}$$

Similarly the waveform parameters vector equals to $\theta_k = T$ Gaussian LFM pulse:

$$\tilde{s}(t) = \left(\frac{1}{\pi T^2}\right)^{1/4} \exp\left(-\left(\frac{1}{2T^2} - j\mu\right)t^2\right) \tag{2.47}$$

$$R(\theta_k) = \begin{bmatrix} \frac{c^2T^2}{2n} & \frac{-c^2\mu T^2}{2\pi f_c n} \\ \frac{-c^2\mu T^2}{2\pi f_c n} & \frac{c^2}{(2\pi f_c)^2 n}\left(\frac{1}{2T^2} + 2\mu^2T^2\right) \end{bmatrix} \tag{2.48}$$

where in this case $\theta_k = [T, \mu]$ with μ denoting the chirp rate and T the pulse duration. The three different waveform classes create a waveform library and allow greater flexibility on the transmitter. The transmitter choses the best waveform to emit based on its optimization problem.

A collaborative strategy between two radar platforms is also presented to enhance the performance of the target tracking precision. The idea is that the two radars will exchange information in real time trying to minimize the ambiguities of their decisions and optimize the choice of the next transmitted waveform. The scenario includes a distance-dependent SNR meaning that the collaborative radars will operate under different SNR conditions, therefore the selection of the next transmitted waveform will be made separately by each radar. More specifically the two radars will share the estimation of the target state and covariance as this is computed in the observation update step of the Kalman filter according to:

$$X_{k|k} = X_{k|k-1} + K_k \left[Y_k - H_k X_{k|k-1} \right] \tag{2.49}$$

$$P_{k|k} = \left[I - K_k H_k \right] P_{k|k-1} \tag{2.50}$$

where K denotes the Kalman gain and Y the measurement. Given the fact that the estimations of the two radars are represented by Gaussian functions we can fuse these estimations by calculating the product of the two Gaussians and derive a new pdf. The new estimation which will be based on the two separate radar estimations is expected to improve the performance taking advantage of the different positioning of the radars. The estimations of the two radars separately are given by the following probability density functions:

$$p_1\left(Y_{1_k}; X_{1_{k|k}}, P_{1_{k|k}}\right) = \frac{1}{\sqrt{2\pi P_{1_{k|k}}}} exp\left(-\frac{\left(Y_{1_k} - X_{1_{k|k}}\right)^2}{2P_{1_{k|k}}} \right) \tag{2.51}$$

$$p_2\left(Y_{2_k}; X_{2_{k|k}}, P_{2_{k|k}}\right) = \frac{1}{\sqrt{2\pi P_{2_{k|k}}}} exp\left(-\frac{\left(Y_{2_k} - X_{2_{k|k}}\right)^2}{2P_{2_{k|k}}} \right) \tag{2.52}$$

where Y_{1_k} represents the observation vector and $X_{1_{k|k}}$, $P_{1_{k|k}}$ denote the mean and covariance of the target as estimated by the first radar. Y_{2_k}, $X_{2_{k|k}}$ and $P_{2_{k|k}}$ are the equivalent vectors for the second radar. We can now we fuse the information provided by the above estimations by

calculating the product of the two pdfs.

$$\begin{aligned} p_f\left(Y_{1_k}, Y_{2_k}; X_{1_{k|k}}, P_{1_{k|k}}, X_{2_{k|k}}, P_{2_{k|k}}\right) = \\ = \frac{1}{\sqrt{2\pi P_{1_{k|k}}}} exp\left(-\frac{\left(Y_{1_k} - X_{1_{k|k}}\right)^2}{2P_{1_{k|k}}}\right) \times \frac{1}{\sqrt{2\pi P_{2_{k|k}}}} exp\left(-\frac{\left(Y_{2_k} - X_{2_{k|k}}\right)^2}{2P_{2_{k|k}}}\right) \\ = \frac{1}{2\pi\sqrt{P_{1_{k|k}} P_{2_{k|k}}}} exp\left(-\left(\frac{\left(Y_{1_k} - X_{1_{k|k}}\right)^2}{2P_{1_{k|k}}} + \frac{\left(Y_{2_k} - X_{2_{k|k}}\right)^2}{2P_{2_{k|k}}}\right)\right) \end{aligned} \tag{2.53}$$

After we expand the quadratic terms in the exponent we can write the Eq.(2.53) in Gaussian form:

$$p_f\left(Y_{f_k}; X_{f_{k|k}}, P_{f_{k|k}}\right) = \frac{1}{\sqrt{2\pi P_{f_{k|k}}}} exp\left(-\frac{\left(Y_{f_k} - X_{f_{k|k}}\right)^2}{2P_{f_{k|k}}}\right) \tag{2.54}$$

with fused mean and covariance described by:

$$X_{f_{k|k}} = \frac{X_{1_{k|k}} P_{2_{k|k}} + X_{2_{k|k}} P_{1_{k|k}}}{P_{1_{k|k}} P_{2_{k|k}}} \tag{2.55}$$

$$P_{f_{k|k}} = \frac{P_{1_{k|k}} P_{2_{k|k}}}{P_{1_{k|k}} + P_{2_{k|k}}} \tag{2.56}$$

The fused estimation after each pulse will then be fed into the tracker of both radars replacing the estimations $X_{1_{k|k}}$, $P_{1_{k|k}}$, $X_{2_{k|k}}$, $P_{2_{k|k}}$ with $X_{f_{k|k}}$ and $P_{f_{k|k}}$ respectively. The radars will independently generate the waveforms for the next emission according to the control theoretic approach but the new waveforms will now be based on the fused estimation of state and covariance instead of the independent estimations (Fig.2.10).

The tracking error of the adaptive waveform design utilizing the control theoretic approach (section 2.3.5) is now compared to the tracking error of a fixed waveform. We are simulating an underwater scenario where the transmitting platform is located at the beginning of the measurement axis and the target is located at a distance of $300m$ and is moving towards the sonar. The target follows a linear trajectory with an initial velocity of $5m/s$ and acceleration $0.5m/s^2$. The carrier frequency is set at $25KHz$ and the process noise variance is $Q = 0.01$. The signal to noise ratio at $r = 1000m$ distance from the target is $n_{1000} = -30dB$ and for the rest target positions is calculated by $n = (1000/r)^4 n_{1000}$. Kalman filter is utilized for the

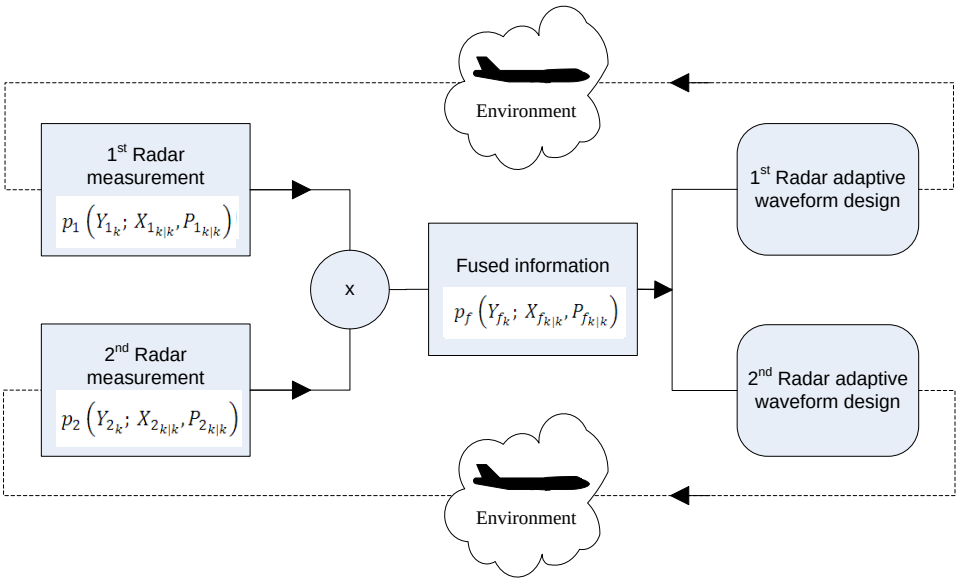

FIGURE 2.10: Block diagram of proposed collaborative strategy.

tracking of the target. The three waveforms described above (Triangular, Gaussian, Gaussian LFM, Eq.(2.43)-Eq.(2.48)) are available in the waveform generator of the radar and their transmitted pulse duration can be adjusted from $10ms$ to $300ms$ with a step of $10ms$ and for the Gaussian LFM waveform the bandwidth of the sweep rate can be adjusted from $-10KHz$ to $0KHz$ with step of $1KHz$. The waveform of the fixed radar is a Triangular pulse with pulse duration $10ms$. The results of the simulation are presented in Fig.2.11-Fig.2.13.

In Fig.2.11 we can see the improvement in the mean square tracking error of the adaptive waveform (especially after the $100m$) compared to the fixed and we can clearly notice the difference in the behaviour of the two waveforms. Although they have similar performance at the stage where the target is approaching the sonar, when the target is accelerating away from the platform the fixed waveform will behave in the same pattern (the error is higher as the target moves away from the sonar) but the adaptive waveform will maintain the low tracking error. Once the radar receives measurements with low noise covariance (which happens as the target gets closer to the radar) the adaptive waveform will maintain the received measurements noise covariance in low levels therefore leading to increased tracking performance compared to the fixed waveform which is particularly obvious in the range of 100-200m. This reveals the dependence of the fixed waveform from the signal to noise ratio when at the same time the adaptive waveform seems to be much less dependent. Fig.2.12

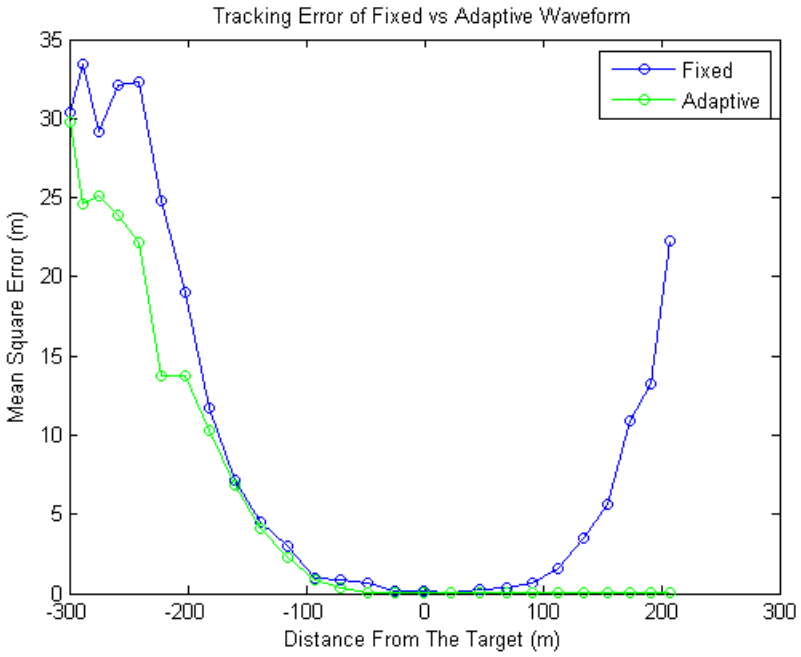

FIGURE 2.11: Tracking Error of Fixed vs Adaptive Waveform.

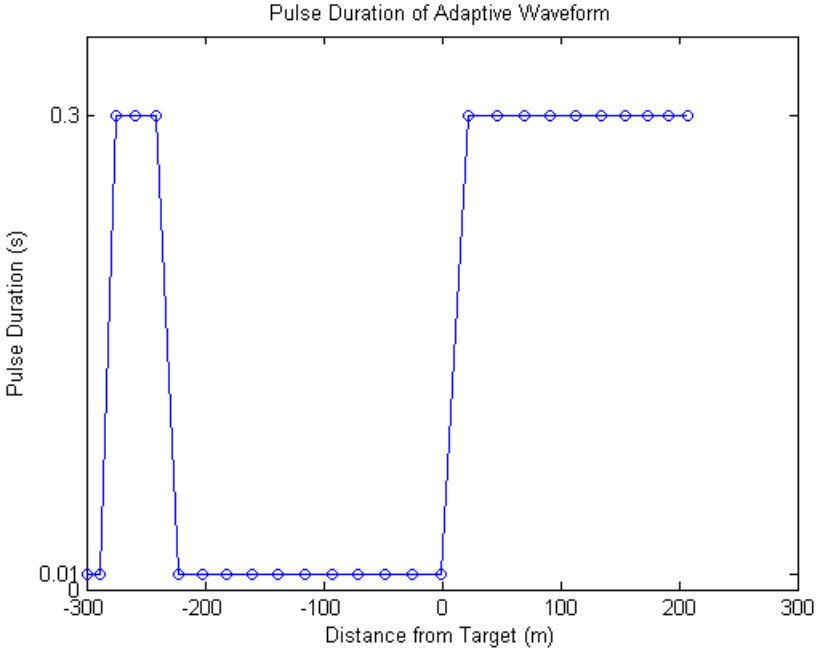

FIGURE 2.12: Pulse Duration of Adaptive Waveform.

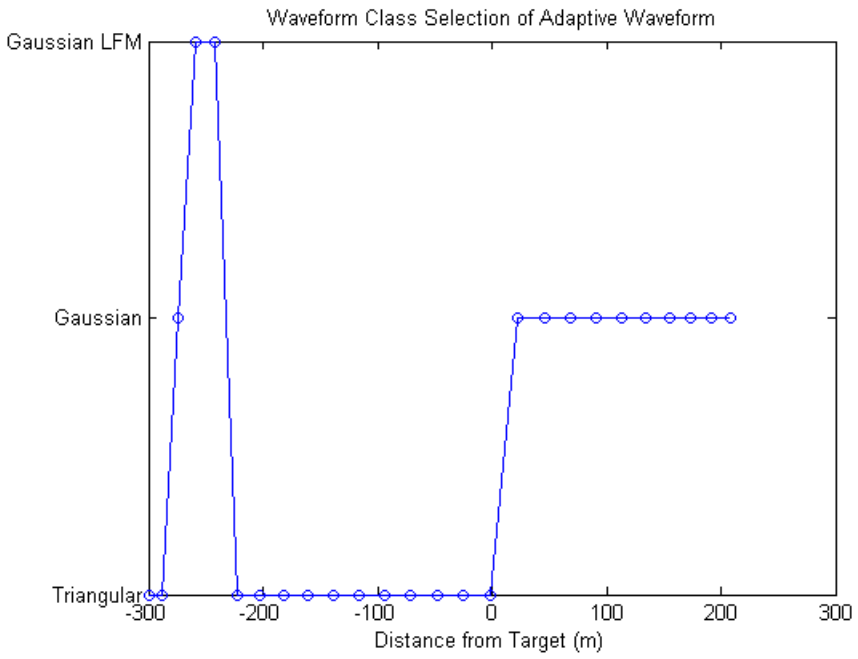

FIGURE 2.13: Waveform Class Selection.

depicts the choice of the pulse duration of the adaptive waveform. After the first stage where we can see the alternately choice of low and high pulse duration, low duration pulse is chosen when the target is approaching and high duration pulse when the target is moving away. Finally, Fig.2.13 shows the choice of the waveform class made at each time step. Again after the first phase where we can see all of the waveforms were used, the Triangular pulse is used when the target is moving toward the sonar and Gaussian pulse when it is accelerating away from it.

The next simulation aims to highlight the enhancement of the performance in a collaborating scenario between two sonar platforms on the target tracking precision as presented previously in Eq.(2.51)-Eq.(2.56). The simulation is set by placing the first sonar at $0m$ and the second at $1000m$. Both are using the adaptive waveform design based on the control theoretic approach and the target is placed at $-500m$ moving toward the two platforms. The results of the simulation are presented in Fig.2.14. The individual performance of the two sonars when they are not sharing data is depicted and is compared to the performance of the collaborative strategy. The collaborative strategy combines the estimations of the two sonars and the result is a significant improvement of the tracking performance of the non-collaborative

scenario. Although a quick look on the results may suggest that the strategy is reduced simply in 'switching' from one radar to another, a more careful review will show us that the moment of 'switching' is not easy to determine. Although the 'switching' point would be expected to be in the middle of the distance between the radars, we can see that this is not the case. The reason is that the 'switching' point mainly depends on the levels of the received measurements noise covariance of the two radars and not on their relative distance therefore their collaboration is vital to the improvement of the tracking precision.

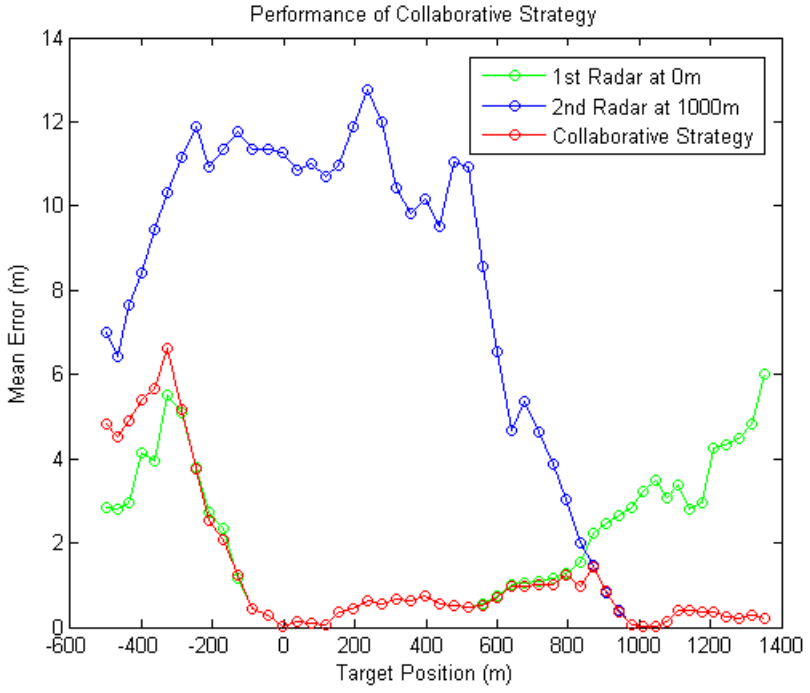

FIGURE 2.14: Mean Error of Collaborative vs non-Collaborative strategy.

2.6 Summary and Conclusions

To summarize, the echo-location system of the bats proves how the interaction with the environment can improve the chances of a successful navigation, prey pursuit and object classification. This behaviour is introduced to radar systems with the growing concept of Cognitive Radar. The waveform design techniques that are used to adapt the transmitted waveform to the environment of the radar by utilizing the feedback loop (i.e. the received

echoes) are presented. Those methods are categorized and analysed. Out of the above methods, the control theoretic approach which predicts the measurement error of the next illumination is applied to show the improvement of the tracking performance on an adaptive LFM waveform compared to the transmission of a fixed LFM waveform. We also present a waveform generator that is provided with a library of three classes of adaptive waveforms. This is an added degree of freedom that allows the transmitter not only to adapt the parameters of the waveform but also choose the type of waveform that will result in improved performance. Finally, to highlight the benefits of communication between radars we propose a strategy where radars exchange information leading to better results in the tracking accuracy.

Chapter 3

Adaptive Waveform Design under Power Constraints for Search and Track

3.1 Introduction and Objectives

In a complex system where multiple sensors are present or even in systems with a single sensor able to perform more than one functions, sensor management techniques are undoubtedly required. The need for sensor management arises when multiple sensors compete over the same limited resources and only one or some of them can be allowed to utilize the means required to perform their function. The resources that are to be considered can vary but the most common are the spectrum availability and the computational power that when neglected can lead to high interference and performance degradation respectively. Another case where sensor management techniques are useful is when a sensor has more than one type of operation but they cannot be carried out at the same time or when the action to be taken has to be bounded in space and/or time. For example, this can be the case if a sensor can perform both surveillance and target classification and sensor management decides which of the functions to be performed and where. Sensor management aims to optimise the distribution of resources between the sensors in the same system and optimise the selection of sensor actions according to the radar mission.

The problem considered in this chapter is a ground based radar responsible for a surveillance area that can perform two actions but just one at a time. Search for new targets or track an existing. A sensor management technique inspired by the study carried out in [13] is used that divides the time between the two modes and for each mode selects the appropriate action for the sensor. The sensor management algorithm should divide the time between the two modes satisfying the dynamic input by the operator and for each mode select the appropriate action for the sensor. Then an adaptive waveform design method will adjust the transmitted waveform maximizing the probability of detection when the radar operates in search mode and minimizing the tracking error in track mode.

The objective of this analysis is to propose an adaptive waveform design to improve the system's performance within the sensor management problem and ensure that the total transmitted power is reduced compared to fixed waveform. In particular, the adaptive waveform design adjusts the pulse duration and peak power of the transmitted Gaussian pulse. In track mode the pulse duration is adjusted based on the target impulse response leading to minimization of the tracking error and the peak power of the transmitted waveform is reduced when it does not affect the performance of the tracker. The power saved in track mode as a result of the reduction of the peak power is used to improve the performance of searching. When the saved power is sufficient, the pulse width is increased in order to achieve maximum probability of detection.

The approach presented here builds on the approaches described in the literature and the specific contributions are:

- A simple adaptive waveform design is combined with sensor management techniques leading to enhanced performance.
- A power saving method is proposed which reduces the transmitted peak power in tracking when it is feasible and allocates the saved power in search mode for increased probability of detection.

3.2 Sensor Management and Adaptive Waveform Design

The radar of our study is located at the origin of a circular two- dimensional surveillance area with radius R_s and the sensor is able to illuminate the area using M beams denoted by m_i, $i = 1, ..., M$ with each one having its own beam width Δn_m. The beams cover the whole area without overlapping, therefore dividing the surveillance area in M cells denoted by A_i, $i = 1, ..., M$, equally to the number of the beams, but only one beam can be used at each time step k. The radar setup is illustarted in Fig.3.2. The sensor uses one beam to illuminate each cell and the waveform transmitted by the radar is a Gaussian CW pulse where the pulse duration $T \in [T_{min}, T_{max}]$ can be adjusted. Each beam is responsible for illuminating only a specific cell and can be used by both the search and track modes of the radar. In search mode the radar will illuminate a selected cell in order to detect new undetected targets and at the same time update the state of already detected targets in this cell. In track mode the aim is to update the state of a specific target. The sensor illuminates the cell which contains the target selected and a tracking algorithm updates its state. The selection of the cell to be illuminated in the search mode or of the target in the track mode at each transmission is made by the sensor management algorithm, creating a sequence of beams and radar modes in order to satisfy the requirements of the operator.

The operator defines how much time is allocated on the search and track modes of the radar by specifying the desired ratio of time that will be spend on the tracking mode. The desired ratio is selected based on the operators needs, radar mission and can be dynamic. When the desired ratio denoted by $\Gamma \in [0, 1]$ is 0 then only search mode is required, while on the other hand 1 means that only tracking will be performed. The real ratio of time spent on track to the overall time at time step k is defined by:

$$\gamma_k = \frac{T_k^t}{T_k^t + T_k^s} \tag{3.1}$$

where T_k^t and T_k^s is the total time spend on track and search mode respectively up to time step k. In order to choose the radar mode for the next transmission the real ratio γ_k is compared to the desired ratio Γ. If it is lower the track mode is selected, otherwise the search mode is chosen maintaining the real ratio γ_k as closer to the desired ratio Γ as possible.

The probability of detection P_d of a target in range r can be calculated by [55]:

$$P_d(r) = \frac{e^b}{1+e^b},\ b = \frac{10^{SNR_{dB}(r)/10} - a}{0.12a + 1.7},\ a = ln\left(0.62/P_{fa}\right) \tag{3.2}$$

where P_{fa} represents the probability of false alarm. The SNR of the targets located in range r is calculated according to the formula[13]:

$$SNR_{dB}(r) = 40log_{10}\frac{r_{50}}{r} + SNR_{dB}(r_{50}) \tag{3.3}$$

where $SNR_{dB}(r_{50})$ is the required signal to noise ratio in order to achieve probability of detection $P_d = 0.5$ and r_{50} represents the distance where it is achieved. $SNR_{dB}(r_{50}) \approx 11.25$ [55] for desired probability of false alarm $P_{fa} = 10^{-6}$.

3.2.1 Track Mode

When track mode is selected, we need to decide which target will be illuminated. Assume that N is the number of targets already detected and are denoted by n_j with $j = 1, ..., N$. The entropy of a d-dimensional Gaussian random variable x is given by [13]:

$$\mathcal{H}(x) = \frac{d}{2}ln(2\pi e) + \frac{1}{2}ln|P| \tag{3.4}$$

where P is the covariance matrix of the target state. The information gain is defined as the variation in entropy after the potential new measurements from the radar are taken into account:

$$\mathbf{I} = \mathcal{H}\left(X_k \mid [Y_1 \dots Y_{k-1}]\right) - \mathcal{H}\left(X_k \mid [Y_1 \dots Y_{k-1}], \breve{Y}_k\right) \tag{3.5}$$

with $\breve{Y}_k$ representing the uncertainty of whether a measurement is generated at time step k depending on the detection or not of a target. Introducing the expected probability of detection of the target $\hat{P}_d$ we can expand the second term of the information gain $\mathbf{I}$:

$$\begin{aligned}\mathcal{H}\left(X_k \mid [Y_1 \dots Y_{k-1}], \breve{Y}_k\right) =& \hat{P}_d\mathcal{H}(X_k \mid [Y_1 \dots Y_{k-1}], Y_k) + \\ & \left(1 - \hat{P}_d\right)\mathcal{H}(X_k \mid [Y_1 \dots Y_{k-1}])\end{aligned} \tag{3.6}$$

Substituting Eq.(3.4) and Eq.(3.6) into the information gain Eq.(3.5) and replacing the covariance matrix P according to the Kalman filter Eq.(2.13)-Eq.(2.17) we result to the following expression of the information gain of target j at k^{th} time t_k [13]::

$$\mathbf{I}_{j,k} = \frac{\hat{P}_d}{2} ln\left(\frac{|P_{k|k-1}|}{|P_{k|k}|}\right) = \frac{\hat{P}_d}{2} ln\left(\frac{|H_k P_{k|k-1} H_k^T + R_k|}{|R_k|}\right) \tag{3.7}$$

where $\hat{P}_d$ is the expected probability of detection, $P_{k|k}$ is the covariance matrix of the expected target state as calculated by the Extended Kalman Filter (EKF), H_k the linearized measurement matrix, R_k is the measurement error covariance matrix and T the transpose. The target selected for tracking at time t_k is the target with the maximum information gain [13]:

$$n_{j,k} = \arg\max_j \mathbf{I}_{j,k} \tag{3.8}$$

The cell $A_{i,k}$ that is illuminated is the cell that contains the chosen target $n_{j,k}$.

As already described in Chapter 2 and based in the Control theoretic approach, the choice of the pulse duration T_k^* for each illumination that minimizes the expected mean-square error of the tracking is made according to:

$$T_k^* = \underset{T\in[T_{min},T_{max,k}]}{\arg\min} \; Tr\left\{P_{k|k}(T_k)\right\} \tag{3.9}$$

$T_{max,k}$ denotes the maximum pulse width for the time instant k with $T_{max,k} \leqslant T_{max}$. The value of $T_{max,k}$ is explained in the following paragraphs.

We now consider the problem of power saving by adjusting the peak power P_t. The probability of detection P_d for constant P_{fa} depends solely on the SNR as described by Eq.(3.2). SNR can be described by the radar equation expressed in dB values, as derived by Eq.(2.2) when zero receiver losses are assumed (L_r = 0), according to:

$$\begin{aligned} SNR_{dB} =& P_{t_{dB}} + T_{dB} + 2G_{dB} + 2\lambda_{dB} + b_{dB} - \\ & (30log(4\pi) + k_{dB} + T_{e_{dB}} + F_{n_{dB}} + 4r_{dB}) \end{aligned} \tag{3.10}$$

where T_{dB} denotes the pulse duration, $P_{t_{dB}}$ the peak transmitted power, G_{dB} the antenna gain, λ_{dB} the wavelength, b_{dB} the radar cross section, k_{dB} the Boltzmann's constant, $T_{e_{dB}}$

the effective noise temperature, $F_{n_{dB}}$ the noise figure and r_{dB} is the distance from the target. Assuming that every factor of Eq.(3.10) remains constant during a single illumination (even the pulse width T_{dB} will not be altered until the next transmission), a reduction of N_{dB} from the peak power $P_{t_{dB}}$ will result in a decrease of N_{dB} on the SNR_{dB}. Although reducing the peak power $P_{t_{dB}}$ will in turn result in decrease on the probability of detection P_d, when the SNR_{dB} is high we can reduce the peak power $P_{t_{dB}}$ having only an insignificant effect on the probability of detection P_d as shown in Fig.3.1. Fig.3.1 reveals that for $SNR_{dB} \geqslant 15.6$ the probability of detection is $P_d \geqslant 0.999$. In this case, when the predicted $\hat{SNR}_{dB}$ is higher than $15.6dB$ we can save $N_{dB} = \hat{SNR}_{dB} - 15.6$ in peak power $P_{t_{dB}}$ and at the same time achieve $P_d \geqslant 0.999$.

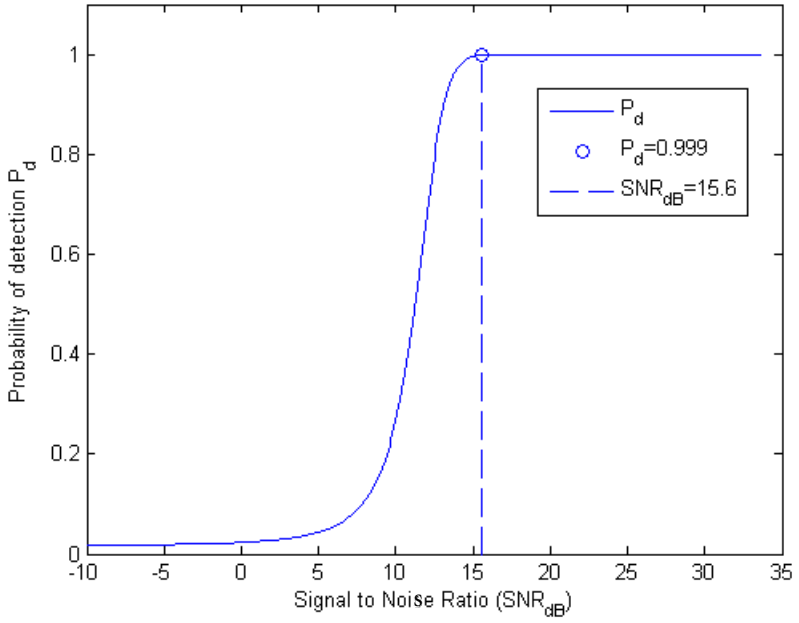

FIGURE 3.1: P_d as a function of SNR_{dB} for $P_{fa} = 10^{-6}$.

The adjusted peak power $P^*_{t_{dB},k}$ is selected according to:

$$P^*_{t_{dB},k} = \begin{cases} P_{t_{dB}} - \left(\hat{SNR}_{dB_{j,k}} - 15.6\right) & , \hat{SNR}_{dB_{j,k}} > 15.6 \\ P_{t_{dB}} & , \text{otherwise} \end{cases} \tag{3.11}$$

where $P_{t_{dB}}$ denotes the peak power of the fixed waveform and $\hat{SNR}_{dB_{j,k}}$ is the predicted $\hat{SNR}_{dB}$ at time t_k of the selected target n_j according to Eq.(3.8).

Both the selection of the pulse duration T_k^* and peak power $P_{t,k}^*$ affects the total transmitted power denoted by $W_k^* = P_{t,k}^* T_k^*$ (in watts). The transmitted power for the fixed waveform is $W_f = P_t T_f$ where $T_f \in [T_{min}, T_{max}]$ represents the fixed pulse duration. When $T_k^* > T_f$ in combination with low or no reduction in the peak power the adaptive design results in increased power consumption. In this case the excess in power can be covered using the already saved power but when the saved power is not enough the adaptive pulse duration T_k^* has to be bounded. We denote the total saved power at time t_{k-1} by $W_{T,k-1}$ and $T_{max,k}$ is expressed by:

$$T_{max,k} = min\left(\frac{W_{T,k-1} + W_f}{P_{t,k}^*}, T_{max}\right) \tag{3.12}$$

Eq.(3.12) ensures that the total power consumption of the adaptive design will always be lower or equal to the total power consumption of the fixed waveform. The total saved power after this illumination $W_{T,k}$ is the sum of the previously total saved power ($W_{T,k-1}$) and the power saved on the current illumination ($W_f - W_k^*$) as described by:

$$W_{T,k} = W_{T,k-1} + (W_f - W_k^*) \geqslant 0 \tag{3.13}$$

3.2.2 Search Mode

When search mode is activated the sensor management defines which cell will be illuminated. Search mode is used in order to detect new targets that either have already been in the surveillance area but were undetected or have just arrived. The goal is to detect the most possible targets at every illumination. To achieve this every cell A_i of the surveillance area is characterized by the expected number of undetected targets $\Lambda(A_i, t_k)$ at each time instant k. The arrival rate of new targets is assumed to follow Poisson distribution similarly to [13] and can be different from cell to cell denoted by $\mu^{A_i}(sec^{-1})$. Prior information is taken into account to calculate the expected probability of detection in each cell $P_d^{A_i}$. The expected number of undetected targets in cell A_i before the illumination t_k^- is calculated by:

$$\Lambda(A_i, t_k^-) = \mu^{A_i}(t_k - t_{k-1}) + \Lambda(A_i, t_{k-1}^+) \tag{3.14}$$

with t_{k-1}^{+} representing the time after the illumination on the previous time step. If the cell is illuminated the expected number of undetected targets in this cell is updated according to:

$$\Lambda(A_i, t_k^{+}) = \begin{cases} \Lambda(A_i, t_k^{-}) - L & , L \text{ targets detected} \\ \Lambda(A_i, t_k^{-})(1 - P_d^{A_i}) & , \text{no detections} \end{cases} \tag{3.15}$$

with t_k^{+} representing the time instant after the observations. In case the cell is not selected for illumination the expected number of undetected targets remains constant. The cell that maximises the expected number of newly detected targets is illuminated at time t_k as described by the following cost function similarly to [13]:

$$A_{i,k} = \arg\max_{A_i} P_d^{A_i} \Lambda(A_i, t_k^{-}) \tag{3.16}$$

The improvement of the probability of detection P_d in search mode is achieved through the adaptive pulse duration of the waveform while the peak transmitted power remains constant. According to the radar equation (Eq.2.2 with $L_r = 0$ and $B = 1/T$) the SNR is proportional to the pulse duration of the waveform:

$$SNR = \frac{T P_t G^2 \lambda^2 b}{(4\pi)^3 k T_e F_n r^4} \propto T \tag{3.17}$$

From Eq.(3.2) we notice that an increase of the SNR results in higher P_d and therefore from Eq.(3.2), Eq.(3.17) we realize that in order to maximize our probability of detection the highest available pulse width has to be transmitted. Taking into consideration the power constraints and the total saved power $W_{T,k-1}$ the maximum pulse width that can be transmitted is calculated similar to Eq.(3.12):

$$T_k^{*} = min\left(\frac{W_{T,k-1} + W_f}{P_t}, T_{max}\right) \Rightarrow T_f \leqslant T_k^{*} \leqslant T_{max} \tag{3.18}$$

therefore the choice of T_k^{*} always results to better or equal P_d compared to the fixed waveform. The total saved power is updated according to Eq.(3.13).

The proposed method for sensor management and waveform design is in short presented here:

while $radar\ operates$ **do**

$\Gamma \leftarrow \gamma \in [0,1]$ [input by the operator]

$Mode \leftarrow Search\ or\ Track$

if $Mode = Search$ **then**

$A_{i,k} \leftarrow \arg\max_{A_i} P_d^{A_i} \Lambda(A_i, t_k^-)$ [Eq.(3.16)]

$T_k^* = min\left(\frac{W_{T,k-1}+W_f}{P_t}, T_{max}\right)$ [Eq.(3.18)]

else $\{Mode = Track\}$

$n_{j,k} \leftarrow \arg\max_j \mathbf{I}_{j,k}$ [Eq.(3.8)]

$T_k^* \leftarrow \arg\min_{T\in[T_{min},T_{max}]} Tr\left\{P_{k|k}(T_k)\right\}$ [Eq.(3.9)]

if $\hat{SNR}_{dB_{j,k}} > 15.6$ **then**

$P^*_{t_{dB},k} \leftarrow P_{t_{dB}} - \left(\hat{SNR}_{j,k} - 15.6\right)$ [Eq.(3.11)]

else

$P^*_{t_{dB},k} \leftarrow P_{t_{dB}}$

end if

end if

end while

It is immediately realised through the above algorithm that the proposed adaptive waveform approach has a negative impact on the computational complexity of the system. Whether the expected improvement in the performance can outbalance the additional computational cost is to be assessed by the needs and capabilities of each system separately, although the constant advances in technology allow the utilization of more complex concepts with high efficiency.

3.3 Implementation and Results

The adaptive waveform design and sensor management techniques discussed in the previous sections will now be applied in a simulated scenario for Gaussian CW pulse as described by Eq(2.45). The aim of the radar is to effectively search and track in the surveillance area according to the input from the operator.

We consider our radar to be in the centre of a circular two dimensional surveillance area with radius R_s = 200km. The area is divided in 10 cells of equal size and each one of them is covered by the respective beam with beam width Δn_m = 36°. At the beginning of the simulation, cells 1-6 already contain a target each which is positioned randomly inside the cell. During the simulation more targets are generated in each cell following a Poisson distribution with arrival rate $\mu^{A_i}(sec^{-1})$ expressed by:

$$\mu^{A_i} = \begin{cases} 0.02 & \text{, i=1,2,3} \\ 0.01 & \text{, otherwise} \end{cases} \tag{3.19}$$

meaning that the first 3 cells expect double the amount of targets to appear than the rest of the cells. Similar to the initial targets, the new targets are placed in random positions inside the cell. Position and velocity on both axes of the Cartesian coordinates describe the target state represented by vector $X = [x, v_x, y, v_y]^T$ which evolves in time linearly as described in Section II. The measurement vector consists of the range r and radial velocity v_r of the target $Y = [r, v_r]^T$ therefore requiring the non linear measurement function:

$$h(X_k) = \begin{bmatrix} \sqrt{x^2 + y^2} \\ \sqrt{v_x^2 + v_y^2} \end{bmatrix} \tag{3.20}$$

The maximum velocity of the targets on each direction is set to $v_{max} = 300m/s$.

Each cell is also described by the adaptive pulse duration of its beam $T^{A_i}(sec \cdot 10^{-5})$ as expressed by:

$$T^{A_i} \in \begin{cases} [0.2, 0.4] & \text{, i=1...7} \\ [0.4, 0.6] & \text{, otherwise} \end{cases} \tag{3.21}$$

In the case of the fixed waveform the pulse duration is set at 3 and 5 $sec \cdot 10^{-5}$ respectively. Lastly, the range from the sensor on each cell where the probability of detection equals to P_d = 0.5 can vary. We denote this distance by $r_{50}(km)$ and is described by:

$$r_{50}^{A_i} = \begin{cases} 1.2 & \text{, i=1...5} \\ 1.4 & \text{, otherwise} \end{cases} \tag{3.22}$$

The combination of the different characteristics attributed to the cells ($\mu^{A_i}, T^{A_i}, r^{A_i}$) creates an inequality among them and therefore we expect some cells to be more often illuminated than others based on their dynamics as described above.

At the beginning of the simulation we assume that no target is detected. For that reason the first mode of the radar is the search mode and will continue to be until at least one target is detected. This is because track mode cannot be initiated when there are no detected targets. While in search mode, sensor management as presented in the previous section (Eq.(3.16)) will select the cell for illumination. The pulse bandwidth can be adjusted aiming to the maximization of the SNR which in turn will lead to maximum probability of detection P_d (Eq.(3.18)). When the tracking mode is in operation, the target to perform tracking is selected according to Eq.(3.8). Extended Kalman filter is used due to the non linearity of the measurement function h which is replaced by the linearized measurement matrix defined by:

$$H_k = \frac{\partial h}{\partial x}\Big|_{x=X_{k|k-1}} \tag{3.23}$$

We assume that there is no association problem and each radar measurement updates the track of the corresponding target. The pulse duration is adapted as described by the Control theoretic approach (Eq.(3.9)) while we investigate the possibility of reducing the peak transmitted power (Eq.(3.11)).

The time interval between successive steps is set at $\Delta T = 1sec$. For the first 40 seconds the ratio Γ is set to $\Gamma = 0.3$ meaning that we are more interested in detecting rather than tracking when the operation begins and for the rest of the simulation is set at $\Gamma = 0.6$. Fig.3.2 presents the surveillance area and the cells that is divided.

In Fig.3.3 we can see in detail the mode and cell chosen by the sensor management during the simulation for both the fixed and adaptive waveform. As expected by the properties assigned to the cells, the first 6 cells gather most of the interest. Although the graphs look similar, there are differences caused by the adaptive pulse duration but most importantly the adaptive waveform results to more detections than the fixed waveform (17 instead of 13 out of 19 targets in total). Fig.3.4 depicts the total saved power compared to the fixed

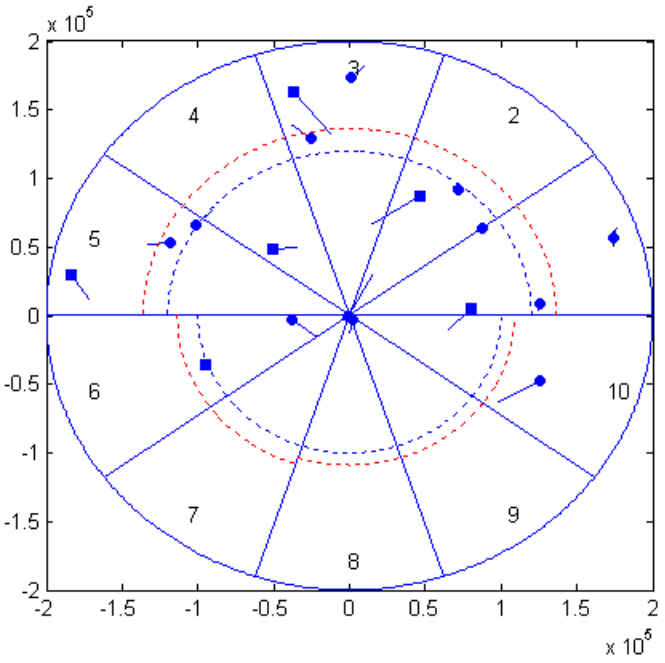

FIGURE 3.2: Targets in surveillance area. The dotted line represents the range where the probability of detection is P_d = 0.5 (blue for fixed, red for adaptive waveform when T_k^* = T_{max}). The initial position of the targets is represented by the blue squares (existing targets) and circles (arrived during the simulation). The line next to them represents their trajectory.

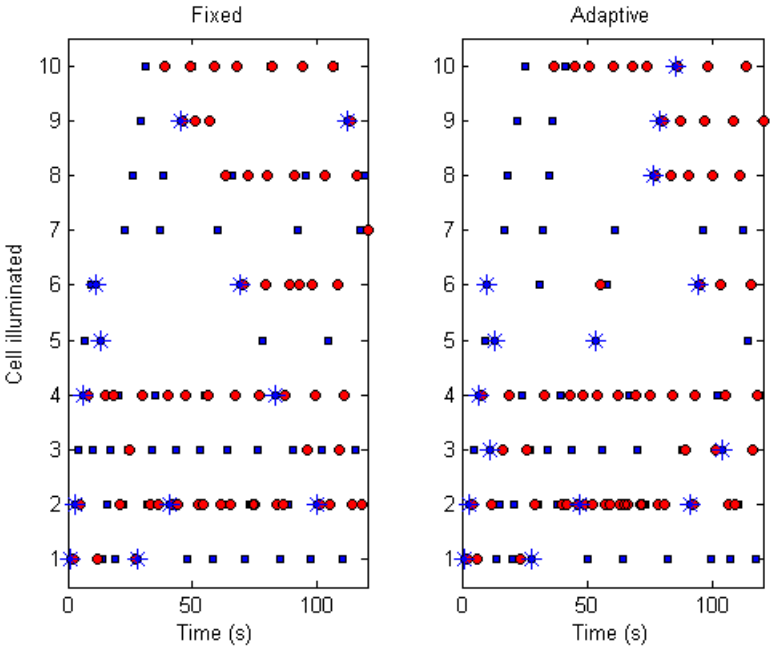

FIGURE 3.3: Cell illuminations. Blue square for search mode and red circles for track. The asterisk denotes that one or more new targets have been detected.

waveform as described by Eq.(3.13). By the end of the simulation we have saved power equal to approximately 23 fixed pulses.

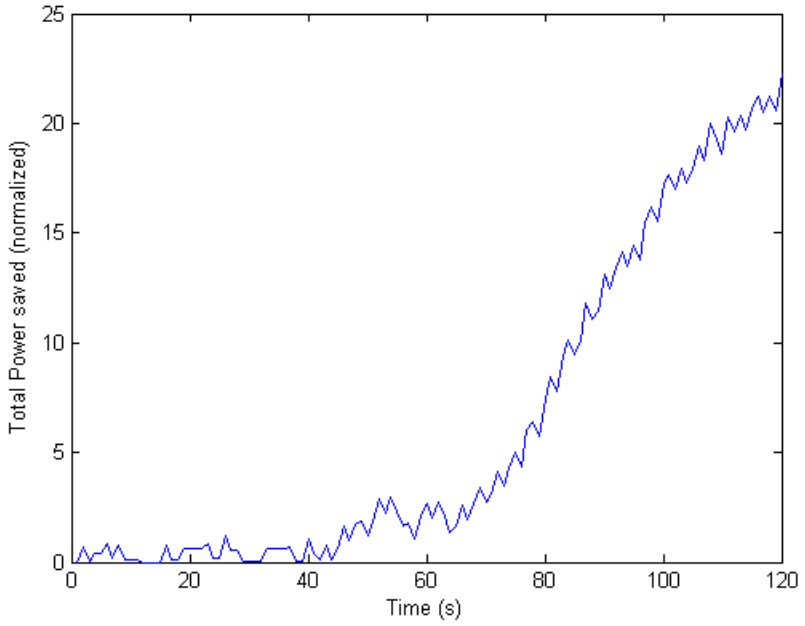

FIGURE 3.4: Total Power saved by the adaptive waveform, normalized to the power of a fixed pulse with $T_f = 0.3sec \cdot 10^{-5}$.

The improvement in the performance is clear on the following figures. Fig.3.5 shows the improvement of the average probability of detection P_d for every target when the adaptive waveform design is implemented (Eq.(3.18)). Some targets are close to the radar and P_d is already at its maximum but for the rest we notice a significant improvement. Fig.3.6 depicts the average tracking error of each target for both fixed and adaptive waveform. We notice the improvement in the tracking error as a result of the adjusted pulse duration (Eq.(3.9)).

3.4 Summary and Conclusions

To summarize, in this chapter a sensor management algorithm which allocates time between search and track modes and specifies the cell or target for illumination has been combined with adaptive waveform design techniques for improved radar performance. The adaptive waveform design achieves higher probability of detection as well as minimizes the tracking

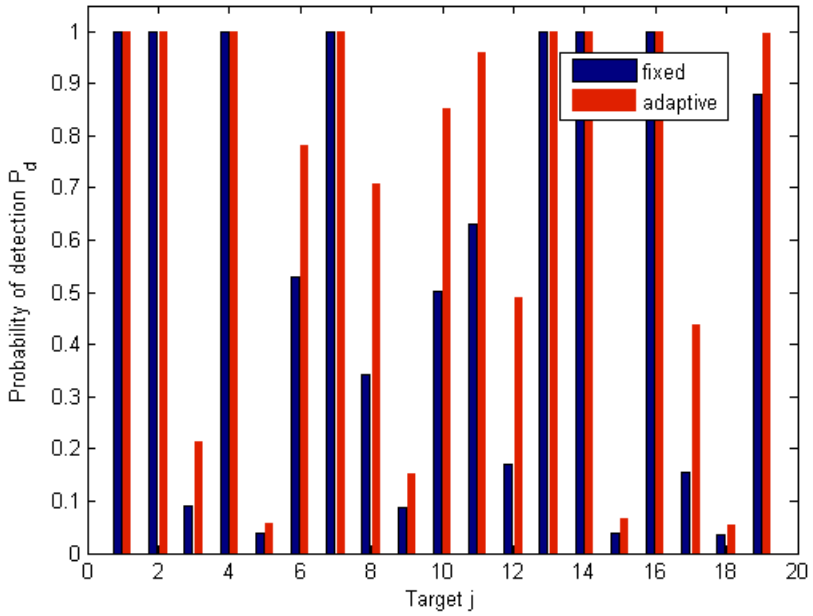

FIGURE 3.5: Mean P_d per target for adaptive vs fixed waveform.

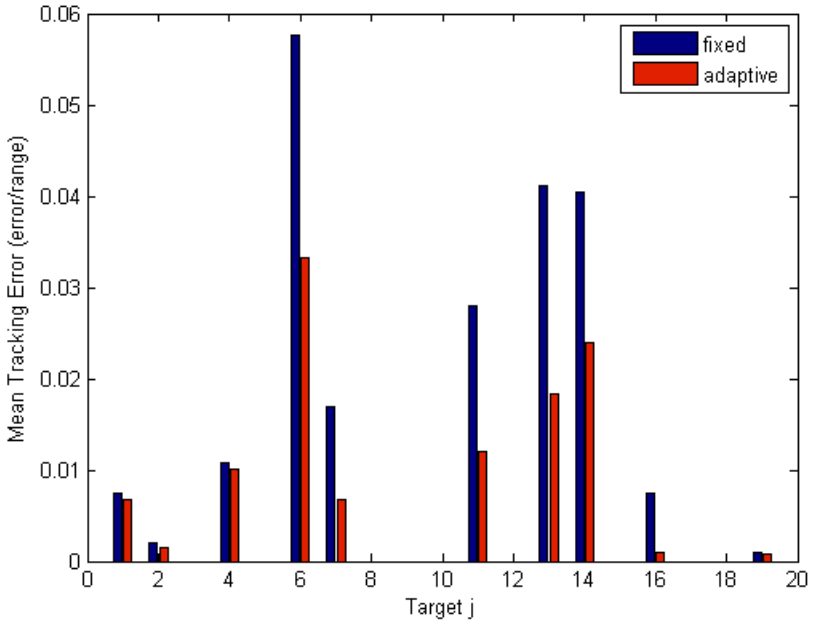

FIGURE 3.6: Mean tracking error per target.

error by adjusting the pulse duration of the transmitted waveform under a constraints on the total transmitted power. Power is saved by reducing the peak power of the waveform when the performance of the tracker is not affected and is allocated on the transmission of longer pulses to increase the probability of detection during search As a result, the total transmitted power of the adaptive waveform is reduced in comparison to total power of the fixed waveform.

Chapter 4

Multi-Sensor Resource Allocation and Waveform Design

4.1 Introduction and Objectives

The evolution of radars has led to radar system that can be composed by more than one sensor either collocated or distributed aiming the maximization of its performance. The number of sensors used by multiple-sensors radars can vary significantly from a small number of sensors (e.g. 2) to a huge sensor network that can include hundreds of sensors. On the other hand, the use of multiple sensors leads to increased system complexity and clever algorithms are required to address the occurring issues.

A fully adaptive multi-sensor system must be capable of allowing each sensor to be able to transmit signals that are optimized for its own mission and based on its own unique condition and environment. At the same time, given the limitations on the available radar resources such as power, time or bandwidth, effective resource allocation methods have to be utilized ensuring that the system is prioritising operations according to its mission and optimizing the overall performance of the radar. As a result, the system is composed by intelligent adaptive sensors that compete over the available radar resources and clever algorithms that have to efficiently allocate the resources to the above sensors.

The objective of this Chapter is to build on the approaches described in the literature for resource allocation and adaptive waveform design and more specifically the contributions are:

- We point out the similarities and the gap in the existing literature among the concepts of resource allocation and adaptive waveform design.
- We propose the development of a joint framework for the implementation of adaptive resource allocation and waveform design on multi-sensor networks and we attempt a first theoretical approach.

4.2 Resource Allocation Literature Review

The resource allocation techniques found in the literature are considering the following resources: i) the mode and the action of the radar itself, ii) the time, iii) the transmitted power, iv) the bandwidth and v) the number and selection of sensors. The allocation of the resources is usually formed as an optimization problem where a metric such as the Mean Square Error (MSE) or the covariance of the target velocity is used as the cost function. Quality of Service (QoS) based Resource Allocation Model (Q-RAM) has also been used for resource management where an function links the quality of different objectives(e.g tracking quality) to the resources to be allocated. Other approaches can consider the problem from a control point of view, formulate the allocation method as a bid auction problem or use fuzzy logic to prioritize the action of the radar. The decision concerning the resources allocation can be done either in a centralized or decentralized method.

The Cramer Rao lower bound (CRLB) has been commonly used as a figure of merit [22] [56] [23] [57] [58] [59]. In [22] the CRLB for the estimation of a target location has been derived in the case of distributed multiple sensors with fixed positions and power is the resource considered. The study formulates two non-convex optimization problems (minimization of the total power budget with constrains on the MSE of a moving target or minimization of the MSE given a power budget) which are solved either through constraints relaxation or domain decomposition methods. Similar approach is taken in [56] for MIMO where apart

from power, bandwidth is also allocated. In this case the non-convex optimization problem is solved through Sequential Parametric Convex Approximation (SPCA). In [23] allocation of power and sensor selection is performed for multiple target tracking. Again the CRLB is used and the optimization problem is solved in two steps using an approximate greedy algorithm [23]. Sensor selection and energy consumption is performed in [58] using an approximation of the CRLB for MIMO resulting to reduced power at the cost of estimation errors while in [59] power is allocated in a sensors network for the minimization of MSE. CRLB is used and the optimization problem is solved using the optimization tool CVX. In the above [22] [56] [23] [58] [59] studies the decision is made in a centralized manner but in [57] a decentralized approach to reduce the computational and communication cost for sensor selection taking into account their battery life is taken. CRLB is calculated and a sub-optimal solution is given to the optimization problem by a local search technique.

The variance unbiased estimate of target velocity is minimized in [60] by selecting the dwell time and the number of observing nodes for a weather radar while in [61] the predicted tracking error covariance matrix through Kalman filters is considered for the allocation of time between the searching and tracking mode for Phased Array Radars keeping all targets in the desired states. Selection of the number of the antennas to exploit spatial diversity taking into account the computational time and minimizing the MSE given by a closed-form solution is performed in [62] for Synthetic Aperture Radar (SAR) while allocation of time and power between the search and track mode of Active Electronically Scanned Array (AESA) radar is proposed in [63] diverting the resources form search to track and vice versa to satisfy the search revisit time (SRT). The maximization of the tracking quality described as an exponential function of both sampling frequency and transmitted power is the objective in [64] where the Q-RAM method has been used subject to limitations on the utilization of the radar processor. Allocating time to the actions of the radar in a control point of view is presented in [65]. The control problem is described using dynamic Finite States Machines and Dynamic Programming is applied to obtain an optimal policy.

An approach for resource allocation where tasks and resource configurations are translated into bids is presented in [66]. The resources that represent the choice of the sensor and the location to be illuminated are allocated through a combinational auction algorithm which

aims to find the optimal object from a finite set of objects. Similar problems related to the optimal selection of a subset can also be solved by using Genetic Algorithms [67], Ant Colony Optimization algorithms[68] or Game Theory [69]. The scheduling and task prioritization problem on a phased array radar has been studied in [70] where fuzzy logic is implemented on the main variables for priority assignment.

4.3 Joint Framework for Resource Allocation and Waveform Design

Apart from the fact that both resource allocation and waveform design techniques (as described in Chapter 2) aim to improve the performance of the radar system we notice that they have more in common. In both cases we deal with the same resources to reach the desired performance. Transmitted power, time (e.g. sampling frequency, pulse duration) and bandwidth are the resources that are most commonly handled in resource allocation and adaptive waveform design problems. This implies that the design of a unifying framework that would perform resource allocation and adaptive waveform design in multi-sensor radars at the same time is feasible. Such framework is missing from the literature and we believe that it can benefit the performance of the radar using the benefits from both methods.

The use of the CRLB as the optimization criterion in both concepts means that it can be the connecting point for a joint framework where resource allocation and waveform design can be simultaneously applied through the derivation of a CRLB that would unify the two concepts. We propose the derivation of a CRLB in a network of sensors where adaptive resource allocation and waveform design will be performed simultaneously. The proposed CRLB will differ from the literature as it will be a function of the available resources to be allocated between the radar network (e.g. time, power, bandwidth, sensor action) as well as a function of the transmitted waveform characteristics (e.g. pulse duration, chirp rate, PRI, carrier frequency). The difficulty of the derivation of such CRLB lies in the fact that each different waveform class produces a different CRLB. This is expected because the CRLB is calculated through the second derivative of the conditional joint probability density function

(pdf) which as we know is a function of the transmitted waveform. That means that for every waveform class a different CRLB has to be derived.

As we have already talked about in the previous Chapters (section 2.3.5), the CRLB provides a lower bound for the MSE of any unbiased estimator. Given a vector parameters θ the unbiased estimate satisfies the following inequality:

$$\mathbf{E}_\theta[(\theta - \bar{\theta})(\theta - \bar{\theta})^T] \geqslant J^{-1}(\theta) \tag{4.1}$$

where $J(\theta)$ is the fisher information matrix, vector parameter θ contains the unknown parameters and $\bar{\theta}$ denotes the mean of measurements.

The following paragraphs will briefly present how the CRLB is used for resource allocation and waveform design separately.

In the resource allocation concept for MIMO radars a formulation of the CLRB is described in [22]. The parameter vector is chosen to be $\theta = [x, y, b]^T$ where (x, y) denotes the position of the target and b is a vector of the target RCS which is different for every sensor $b = [b_{1,1}, b_{1,2}, ..., b_{M,N}]$ with M representing the transmit and N the receive sensors. The fisher information matrix is a 2×2 matrix given by:

$$J(\theta) = \mathbf{E}_{\mathbf{Y}|\theta}\left[\frac{\partial}{\partial\theta}\ln p(Y;\theta)\left(\frac{\partial}{\partial\theta}\ln p(Y;\theta)\right)^T\right] \tag{4.2}$$

where $p(Y;\theta)$ denotes the conditional joint probability density function of the observation $Y = [Y_{1,1}, Y_{1,2}, ..., Y_{M,N}]$ given by:

$$p(Y;\theta) = \frac{1}{(\pi\sigma_w^2)^{\frac{MN}{2}}}\exp\left[-\frac{1}{\sigma_w^2}\sum_{n=1}^{N}\sum_{m=1}^{M}|Y_{m,n}(t) - \sqrt{a_{m,n}p_m}b_{m,n}s_m(t-\tau_{m,n})|^2 dt\right] \tag{4.3}$$

where σ_w^2 denotes the noise variance, $Y_{m,n}$ the received waveform, $a_{m,n}$ the path loss effects, p_m the transmitted power, s_m the transmitted waveform and $\tau_{m,n}$ the propagation time. CRLB in this case is formulated to be a function of the target position and waveform's transmitted power $J^{-1}(\theta, p)$.

On the other hand, in the waveform design concept a standard way to construct the CRLB for single sensor radar is by calculating the Fisher matrix according to:

$$J_{ij}(\theta) = -n\frac{\partial^2\chi(\theta)}{\partial\theta_i\partial\theta_j} \tag{4.4}$$

where n is the SNR, $\theta = [\tau, \omega]$, τ denotes the propagation time, ω the Doppler frequency and χ is the ambiguity function (AF) of the received waveform described by:

$$\chi(\tau,\omega) = \int_{-\infty}^{+\infty} \tilde{s}(t)\tilde{s}^*(t-\tau)e^{-j\omega t}\mathrm{d}t \tag{4.5}$$

In this case we can see that the Fisher matrix and therefore the CRLB depends only on the waveform's characteristics. For a Gaussian LFM waveform for example described by

$$\tilde{s}(t) = \left(\frac{1}{\pi T^2}\right)^{1/4} \exp\left(-\left(\frac{1}{2T^2} - j\mu\right)t^2\right) \tag{4.6}$$

the CRLB can be a function of the waveform's pulse duration T and/or chirp rate μ.

In order to derive a unifying CRLB for both resource allocation and waveform design the first step is the calculation of the appropriate Fisher matrix that will incorporate elements from both approaches. We now select the appropriate parameters $\theta = [\theta_1, \theta_2, ..., \theta_d]^T \in \mathbb{R}^d$ that will create the joint CRLB. Then, the Fisher information matrix will be represented by a $d \times d$ matrix with elements $J_{i,j}$ where $i, j = 1, 2, ..., d$ defined as:

$$J_{i,j}(\theta) = -\mathbf{E}_{\mathbf{Y}|\theta}\left[\frac{\partial^2 \ln \mathrm{p}(Y;\theta)}{\partial\theta_i\partial\theta_j}\right] \tag{4.7}$$

where $\mathrm{p}(Y;\theta)$ denotes the conditional joint probability density function of the observation $Y = [Y_{1,1}, Y_{1,2}, ..., Y_{M,N}]$ with M representing the transmit and N the receive sensors. The transmitted waveform in this case will not be considered fixed and the CRLB will be a function of parameters like power allocation, pulse duration, etc. and will be used to represent the localization MSE.

Suppose that we formulate the received waveform as:

$$Y_{m,n}(t) = \sqrt{a_{m,n}p_m}b_{m,n}s_m(t-\tau_{m,n})e^{-j2\pi\omega_{m,n}t} + w_{m,n}(t) \tag{4.8}$$

where m, n denotes a specific pair of transmitter-receiver, $Y_{m,n}$ the received waveform, $a_{m,n}$ the path loss effects, p_m the transmitted power, $b_{m,n}$ the radar cross section, s_m the transmitted waveform, $\tau_{m,n}$ the propagation time, $\omega_{m,n}$ the frequency shift and $w_{m,n}$ the zero mean noise. In this case the conditional joint probability density function $\mathrm{p}(Y;\theta)$ is described by:

$$\mathrm{p}(Y;\theta) = \frac{1}{(\pi\sigma_w^2)^{\frac{MN}{2}}}\exp\left[-\frac{1}{\sigma_w^2}\sum_{n=1}^{N}\sum_{m=1}^{M}\int\left|Y_{m,n}(t)-\sqrt{a_{m,n}p_m}b_{m,n}s_m(t-\tau_{m,n})e^{-j2\pi\omega_{m,n}t}\right|^2 dt\right] \tag{4.9}$$

and the logarithm is described by:

$$\begin{aligned}\ln\mathrm{p}(Y;\theta) = &-\ln\left((\pi\sigma_w^2)^{\frac{MN}{2}}\right)\\ &-\frac{1}{\sigma_w^2}\sum_{n=1}^{N}\sum_{m=1}^{M}\int\left|Y_{m,n}(t)-\sqrt{a_{m,n}p_m}b_{m,n}s_m(t-\tau_{m,n})e^{-j2\pi\omega_{m,n}t}\right|^2 dt\end{aligned} \tag{4.10}$$

If we analyse the square term we get the following expression:

$$\begin{aligned}&\left|Y_{m,n}(t)-\sqrt{a_{m,n}p_m}b_{m,n}s_m(t-\tau_{m,n})e^{-j2\pi\omega_{m,n}t}\right|^2 =\\ &Y_{m,n}(t)Y_{m,n}^*(t)-\\ &Y_{m,n}^*(t)\sqrt{a_{m,n}p_m}b_{m,n}s_m(t-\tau_{m,n})e^{-j2\pi\omega_{m,n}t}-\\ &Y_{m,n}(t)\sqrt{a_{m,n}p_m}b_{m,n}s_m^*(t-\tau_{m,n})e^{j2\pi\omega_{m,n}t}+\\ &a_{m,n}p_m b_{m,n}^2 s_m(t-\tau_{m,n})e^{-j2\pi\omega_{m,n}t}s_m^*(t-\tau_{m,n})e^{j2\pi\omega_{m,n}t}\end{aligned} \tag{4.11}$$

If we choose our parameter vector to be $\theta = [\tau, \omega]$ then the first term of the above expression, which is purely a function of the measurements, is independent of θ and therefore will be zero after the differentiation (Eq.(4.7)) and the fourth term reduces to $a_{m,n}p_m b_{m,n}^2$ as the waveform is considered to be of unit energy and similarly will be zero after the differentiation. The remaining second and third term take the form:

$$-2\mathrm{Re}\left[Y_{m,n}(t)\sqrt{a_{m,n}p_m}b_{m,n}s_m^*(t-\tau_{m,n})e^{j2\pi\omega_{m,n}t}\right] \tag{4.12}$$

and is the only term of Eq.(4.10) which is dependent of the parameter vector $\theta = [\tau, \omega]$. The Fisher matrix now has the following form:

$$J_{i,j}(\theta) = -\mathbf{E}_{\mathbf{Y}|\theta}\begin{bmatrix} \frac{\partial^2 \ln p(Y;\theta)}{\partial \tau^2} & \frac{\partial^2 \ln p(Y;\theta)}{\partial \tau \partial \omega} \\ \frac{\partial^2 \ln p(Y;\theta)}{\partial \tau \partial \omega} & \frac{\partial^2 \ln p(Y;\theta)}{\partial \omega^2} \end{bmatrix} \tag{4.13}$$

The first derivative with respect to the time delay τ is:

$$\frac{\partial \ln p(Y;\theta)}{\partial \tau} = \frac{2}{\sigma_w^2}\sum_{n=1}^{N}\sum_{m=1}^{M}\int \mathrm{Re}\left[Y_{m,n}(t)\sqrt{a_{m,n}p_m}b_{m,n}\frac{\partial s_m^*(t-\tau_{m,n})}{\partial \tau}e^{j2\pi\omega_{m,n}t}\right]dt \tag{4.14}$$

and the second derivative with respect to the time delay τ:

$$\frac{\partial^2 \ln p(Y;\theta)}{\partial \tau^2} = \frac{2}{\sigma_w^2}\sum_{n=1}^{N}\sum_{m=1}^{M}\int \mathrm{Re}\left[Y_{m,n}(t)\sqrt{a_{m,n}p_m}b_{m,n}\frac{\partial^2 s_m^*(t-\tau_{m,n})}{\partial \tau^2}e^{j2\pi\omega_{m,n}t}\right]dt \tag{4.15}$$

We now take the expectation of the above expression with the expectation of the measurement $Y_{m,n}(t)$ equal to:

$$\mathbf{E}\{Y_{m,n}(t)\} = \sqrt{a_{m,n}p_m}b_{m,n}s_m(t-\tau_{m,n})e^{-j2\pi\omega_{m,n}t} \tag{4.16}$$

and therefore $J_{1,1}(\theta)$ is simplified to:

$$\begin{aligned} J_{1,1}(\theta) &= \mathbf{E}_{\mathbf{Y}|\theta}\left\{\frac{\partial^2 \ln p(Y;\theta)}{\partial \tau^2}\right\} \\ &= \frac{2}{\sigma_w^2}\mathbf{E}\left\{\sum_{n=1}^{N}\sum_{m=1}^{M}a_{m,n}p_m b_{m,n}^2\int \mathrm{Re}\left[s_m(t-\tau_{m,n})\frac{\partial^2 s_m^*(t-\tau_{m,n})}{\partial \tau^2}\right]dt\right\} \end{aligned} \tag{4.17}$$

The first and second derivative with respect to the frequency shift ω are:

$$\frac{\partial \ln p(Y;\theta)}{\partial \omega} = \frac{2}{\sigma_w^2}\sum_{n=1}^{N}\sum_{m=1}^{M}\int \mathrm{Re}\left[Y_{m,n}(t)\sqrt{a_{m,n}p_m}b_{m,n}\partial s_m^*(t-\tau_{m,n})j2\pi t e^{j2\pi\omega_{m,n}t}\right]dt \tag{4.18}$$

$$\frac{\partial^2 \ln p(Y;\theta)}{\partial \omega^2} = \frac{2}{\sigma_w^2}\sum_{n=1}^{N}\sum_{m=1}^{M}\int \mathrm{Re}\left[Y_{m,n}(t)\sqrt{a_{m,n}p_m}b_{m,n}\partial s_m^*(t-\tau_{m,n})j^2 4\pi^2 t^2 e^{j2\pi\omega_{m,n}t}\right]dt \tag{4.19}$$

Similarly, we take the expectation of the expression and the term $J_{2,2}(\theta)$ simplifies to:

$$\begin{aligned} J_{2,2}(\theta) &= \mathbf{E}_{\mathbf{Y}|\theta}\left\{\frac{\partial^2 \ln p(Y;\theta)}{\partial \omega^2}\right\} \\ &= -\frac{8\pi^2}{\sigma_w^2}\sum_{n=1}^{N}\sum_{m=1}^{M} a_{m,n}p_m b_{m,n}^2 \int \mathrm{Re}\left[s_m(t-\tau_{m,n})s_m^*(t-\tau_{m,n})t^2\right]dt \\ &= -\frac{8\pi^2}{\sigma_w^2}\sum_{n=1}^{N}\sum_{m=1}^{M} a_{m,n}p_m b_{m,n}^2 \int \mathrm{Re}\left[t^2\right]dt \end{aligned} \tag{4.20}$$

Finally, for the calculation of $J_{1,2}(\theta) = J_{2,1}(\theta)$ we have:

$$\frac{\partial \ln p(Y;\theta)}{\partial \tau \partial \omega} = \frac{2}{\sigma_w^2}\sum_{n=1}^{N}\sum_{m=1}^{M} \int \mathrm{Re}\left[Y_{m,n}(t)\sqrt{a_{m,n}p_m}b_{m,n}\frac{\partial s_m^*(t-\tau_{m,n})}{\partial \tau} j2\pi t e^{j2\pi\omega_{m,n}t}\right]dt \tag{4.21}$$

$$\begin{aligned} J_{1,2}(\theta) = J_{2,1}(\theta) &= \mathbf{E}_{\mathbf{Y}|\theta}\left\{\frac{\partial^2 \ln p(Y;\theta)}{\partial \tau \partial \omega}\right\} \\ &= \frac{4\pi}{\sigma_w^2}\mathbf{E}\left\{\sum_{n=1}^{N}\sum_{m=1}^{M} a_{m,n}p_m b_{m,n}^2 \int \mathrm{Re}\left[s_m(t-\tau_{m,n})\frac{\partial^2 s_m^*(t-\tau_{m,n})}{\partial \tau^2} jt\right]dt\right\} \end{aligned} \tag{4.22}$$

In order to reach an analytical form of the CRLB we need to insert our transmitted waveform $s_m(t)$ into the above equations and calculate the integrals but is already obvious that the CRLB depends on both the power allocated in each transmitter through p_m and the waveform characteristics through the expression $s_m(t-\tau_{m,n})$.

The calculation of the CRLB as presented here is not in the scope of this study and an analytical expression of the CRLB is recommended to be completed in future studies. Having obtained the analytical expression of the CRLB an optimization problem can be formulated like:

$$\begin{aligned} & \min Tr\left(\left(J_{i,j}(\theta)\right)^{-1}\right) \\ \text{Subject to}: \quad & p_m \le p_{m_{max}}, \qquad \forall m = 1,2,\dots M \\ & p_m \ge p_{m_{min}}, \qquad \forall m = 1,2,\dots M \end{aligned} \tag{4.23}$$

This problem will initially aim to minimize the MSE by allocating power and designing the waveform on all of the sensors. An extension to the above problem can be the sensor selection problem (where only some of the sensors can operate at the same time) and/or the implementation of constrains on the bandwidth depending on the scenario studied.

4.4 Summary and Conclusions

To summarize, the resource allocation and adaptive waveform design in a network of sensors are two different concepts but are using similar tools to achieve their goals. Driven by this observation, we propose the creation of a unifying framework for the simultaneous application of both techniques in a multi-sensor system based on the derivation of a common CRLB that will depend both on the limited system resources (i.e. power, time, etc.) over which the sensors compete and the parameters/class of the transmitted waveform (i.e. PRF, pulse duration, chirp rate, etc.). This will allow the system to allocate resources between the multiple transmitters and at the same time design the waveforms to be transmitted optimizing its mission.

Chapter 5

Conclusions and Further Work

This thesis began by introducing the motivation behind the next step on the evolution of the dynamic radars, commonly known as Cognitive Radar. The ever increasing need for faster, accurate, smart and multifunctional radars due to the modern challenges they face and especially the evolution of their targets who are nowadays equipped with stealth and jamming capabilities combined with the plethora of information available in the radar's environment and the emerge of recent advances in technology, have led to the idea of Cognitive Radar. Cognitive Radar aims to adaptively interact with the environment, gather relevant information and data, communicate with collaborating platforms and by using artificial intelligence techniques along with the already stored databases and previous knowledge to adjust its operations for the enhancement of its performance and completion of its mission.

A natural example of such behaviour is the echo-location system of bats that are some of the few living organisms that are using active sensors to navigate and hunt. Studies have revealed that bats adjust the signals they emit based on the received echoes and their goals. This shows that interaction with the environment and more specifically the feedback loop created through the analysis of the received signal and the emission of the next waveform based on the previous analysis is the critical mechanism that allows bats to be effective on their navigation and hunt. Carrier frequency, pulse duration and pulse repetition frequency are some of the parameters that bats are constantly adjusting in their emitted waves. The benefits

and trade-offs of this adaptive behaviour has been illustrated through a simple scenario on a ground-based radar that implements the way bats hunt.

There are now several approaches on designing adaptive waveforms for a radar system. The Ambiguity Function that provides an insight on the expected range and Doppler resolution of the waveform plays an important role on the adaptation procedure of both the control and the information theoretic approach. The control theoretic approach adapts the waveform based on the prediction of the measurement error covariance matrix while the information theoretic approach based on the maximization of the amount of information the measurements are providing about the target. Arbitrary waveform generators have nowadays allowed the creation of waveforms where both the modulus and the phase can be designed before every transmission but in this way increasing the computational complexity. We have used the control theoretic approach to present the improvement on the tracking performance of an adaptive LFM waveform over a fixed transmission and we have also highlighted the importance of the appropriate choice of the tracking algorithm. We have also constructed a waveform generator that is fed with a library of three different classes of waveforms. In this case the optimization problem includes the choice of the most beneficial waveform along with the adaptation of its parameters. Also, the benefits of collaboration between radars are presented. Further work related to the concept of this chapter is suggested to be the calculation of the measurement noise covariance matrix for more waveforms or families of waveforms. This will enable us to create a broader library of adaptive waveforms, exploit the advantageous characteristics of different classes of waveforms and therefore enabling an increased improvement of the radar performance. The variety and flexibility of transmitted waveforms will also result in improved efficiency of the spectrum management problem.

On the next stage of the work we present an adaptive waveform design method under power limitations that also allows power allocation between the two modes of the radar; search and track. Driven by the fact that adaptive waveform designs can result to increased total transmitted power, we propose a design where the waveform is adapted for increased tracking and searching performance by using reduced power compared to the transmission of fixed waveform. In short, the control theoretic approach is utilized for adjusting the waveform's parameters in tracking and at the same time we reduce the peak transmitted power when the

performance of the tracker is not affected. The saved power is then allocated to increase the probability of detection in search mode. The implementation of the above method results to better tracking and searching performance and reduction on the total transmitted power. The power saving concept of this chapter can be used in future studies with alternative approaches on the allocation of the saved power. This is evident especially when we consider the radar to be a multifunctional system where power is required by more than one functions or in cases where reduced power consumption can lead to extended operational time.

The potential improvements in multi-sensor networks through the creation of a unifying framework for both resource allocation and adaptive waveform design are highlighted in the last part of the thesis. The derivation of a CRLB that would incorporate both concepts and optimize the radar performance is proposed as further work and extension of this thesis. A potential example where this idea can be applied is a network of unmanned aerial vehicles (UAVs) where the dynamic nature of the UAVs supports and enhances the need of adaptive methods. The UAVs should be provided with communication capabilities and therefore be able to form a network for information exchange. Given the common constraints in resources like frequency, bandwidth, power and time, the UAVs add another degree of freedom in the optimization problem with their limited flight time and battery life. The decision process can be made in a centralized manner where each time one of the UAVs will act as a fusion centre that will collect, process and make decisions about the resource allocation and waveform design on every sensor of the network.

Appendix A

Radar Fundamentals

A.1 Unambiguous Range and the Radar Equation

When a pulse is transmitted the radar must wait a sufficient length of time so that the returns from targets at maximum range are back before the next pulse is emitted. This range corresponding to the two-way time delay τ is defined as the maximum unambiguous range:

$$R_u = cT/2 \tag{A.1}$$

In order to make detection, Echo's power P_r should exceed the receiver's power threshold P_{th}. The power density W (Watt/m^2) caused by the transmitter is described by $W = \frac{P_t G}{4\pi R^2}$, where P_t is the transmitted power and G is the antenna gain. Each target illuminated by the radar has its own radar cross section (RCS) $b(m^2)$ defined by $b = \frac{P_{ref}}{W}$. Since P_{ref} is reflected towards the antenna, echo's power density is described by $W_{ref} = \frac{P_{ref}}{4\pi R^2} = \frac{P_t G b}{(4\pi R^2)^2}$. Assuming that the antenna effective aperture A_e is known, $A_e = \frac{\lambda^2 G}{4\pi}$ where λ denotes the wavelength, then the total power delivered to the radar is $P_r = W_{ref} A_e = \frac{P_t G^2 b \lambda^2}{(4\pi)^3 R^4}$. This result shows that the received power is inversely proportional to the fourth power of distance. Assuming that the lowest amount of energy that can be detected is P_{min}, then the maximum range of the

radar R_{max} is calculated by:

$$R_{max} = \left(\frac{P_t G^2 b \lambda^2}{(4\pi)^3 P_{min}} \right)^{1/4} \tag{A.2}$$

A.2 Range Resolution and Doppler Effect

Assume that a pulse is transmitted and after it is reflected on a target it comes back at time delay τ_1. The range calculated by the radar at this time will be $r_1 = \frac{c\tau_1}{2}$. The end of the pulse will be received at time delay $\tau_2 = \tau_1 + T$ and the range calculated by the radar at this point will be $r_2 = \frac{c\tau_2}{2} = \frac{c(\tau_1+T)}{2}$. It is clear that any other targets which range is between r_1 and r_2 will not be separated by the receiver, so the range $r_2 - r_1$ is called Range Resolution and is denoted by:

$$\Delta r = r_2 - r_1 = \frac{cT}{2} = \frac{c}{2B} \tag{A.3}$$

where $B = 1/T$ is the pulse bandwidth.

The Doppler Effect is a physical phenomenon that plays an important role on radars, since it is used to measure the velocity of the target. As known from wave physics, when there is a relative motion between a travelling wave and an observer then the wave frequency received by the observer is different from the original. Measuring Doppler shift radars are able to calculate targets' velocity. It is denoted by ω and equals to:

$$\omega = \frac{2v}{\lambda} \tag{A.4}$$

where v is the target's velocity.

A.3 Radar Waveforms

Choosing the right type of transmitted waveform in a radar system is directly related to its mission. Cost and complexity of each specific type of waveform are also basic factors in the choice of the waveform. Radar systems can use continuous or pulsed waves, with or

without modulation [71]. Modulated waveforms can achieve wider operating bandwidths and improve the range and Doppler resolution of the unmodulated waveforms. Some of the most commonly used waveforms are presented here:

- Frequency Modulation (FM)
  - Linear Frequency Modulation (LFM): the basic idea is to sweep the frequency band B linearly during the pulse duration T as shown in fig.A.1

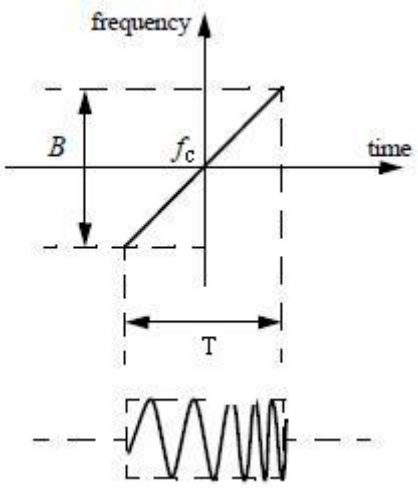

FIGURE A.1: LMF Waveform.

The complex envelope of an LFM waveform can be expressed by:

$$\tilde{s}(t) = \frac{1}{\sqrt{T}}\text{Rect}\left(\frac{t}{\tau}\right)\exp\left[j\pi\mu t^2\right] \tag{A.5}$$

where Rect$(\frac{t}{\tau})$ denotes a rectangular pulse of width T and $\mu = \pm B/T$ is the LMF frequency slope. Compared to an unmodulated pulse the improvement of the range resolution is expressed by the pulse compression rate $CR = \frac{T}{T_{comp}}$ where T is the pulse width of the unmodulated pulse and T_{comp} is the pulse width after the modulation.

  - Costas Coding: the signal is divided in M time slices of equal duration and at any of the M time slice, only one frequency is transmitted and each frequency is used only once as shown in fig.A.2.

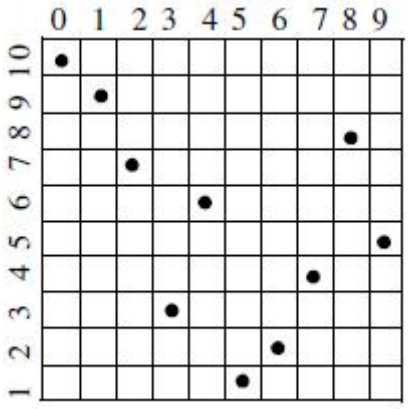

FIGURE A.2: Frequency assignment in a Costas code of length 10.

The frequencies for the subpulses are selected in a random fashion, according to some predetermined rules [72]. The compression ratio (CR) of a Costas code is approximately M.

– Non Linear Frequency Modulation (NLFM): there is no constant rate of frequency change and more time is spent at frequencies that need to be enhanced.

- Phase Coding

  In Phase coding the pulse is divided into M bits of equal duration and each bit is coded with a phase value. The most known codes are Barker Codes, Frank Code, Golomb Codes, Ipatov Code and Huffman Code. Barker Codes are explained below.

  – Barker Codes: One family of binary phase codes that produce compressed waveforms with constant side lobe levels equal to unity is the Barker code. A code of length n is denoted as B_n. Fig.4 depicts the Barker code of length 7, B_7. There are only seven known Barker codes that share this unique property and are listed in fig.A.3.

    Barker Codes can be combined in order to generate longer codes. A B_n code can be used within a B_m to create a code of length mn. The compression ratio of the combined B_{nm} code is equal tomn. As an example, a combined B_{54} is given by B_{54} = $\{11101\ 11101\ 00010\ 11101\}$. However, the side lobes of a combined Barker code autocorrelation function are no longer equal to unity.

- Train of Pulses

Code Symbol	Length	Elements	Side lobe reduction (dB)
B_2	2	10 11	6.0
B_3	3	110	9.5
B_4	4	1101 1110	12
B_5	5	11101	14
B_7	7	1110010	16.9
B_{11}	11	11100010010	20.8
B_{13}	13	1111100110101	22.3

FIGURE A.3: List of Barker Codes.

– Coherent Train of Identical Pulses

Fig.A.4 shows a plot of a coherent pulse train. The pulse width is denoted as T and the PRI is T_{PRI}. The number of pulses in the train is N hence the train's length is $(N-1)T_{PRI}$ seconds. A normalized individual pulse is defined by:

$$\tilde{s}_1(t) = \frac{1}{\sqrt{T}}\text{Rect}\left(\frac{t}{T}\right) \tag{A.6}$$

and the normalized train is expressed by:

$$\tilde{s}(t) = \frac{1}{\sqrt{N}}\sum_{i=0}^{N-1} u_1(t - iT_{PRI}) \tag{A.7}$$

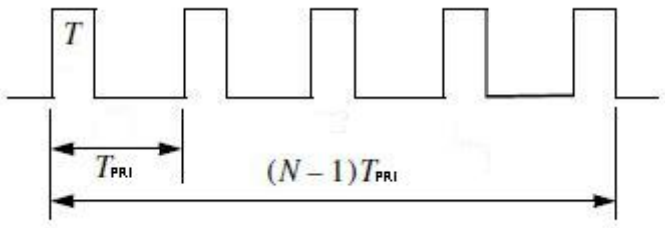

FIGURE A.4: Coherent pulse train of N=5.

- Diversity in the Pulse Train

  Depending on the radar's goal the train of pulses can be composed by diverse pulses. Each pulse can have its own modulation, frequency, even different amplitude. Diversity can also be implemented in the PRI. The PRI can vary between the pulses, changing the train's characteristics and leading to the desired results.

Appendix B

Ambiguity Function

The tool used by radar designers to study the properties of the different waveforms is called Ambiguity Function (AF) and was introduced by Woodward in 1953 [44]. AF is a two-dimensional function of time delay and Doppler frequency showing the distortion of a returned pulse. It is used to determine the range and Doppler resolution for a specific radar waveform and provide useful information about how different waveforms may be suitable for different radar applications. It is defined by:

$$\chi(\tau,\omega) = \int_{-\infty}^{+\infty} \tilde{s}(t)\tilde{s}^*(t-\tau)e^{-j\omega t}\mathrm{d}t \tag{B.1}$$

where τ is the time delay, ω is the Doppler shift and $\tilde{s}$ is the complex envelope of the signal. The AF evaluated at $(\tau,\omega) = (0,0)$ is matched to the waveform reflected from the target. In other words, returns from the desired target are located at the origin of the AF, while AF at nonzero represents returns different from the desired target. For zero Doppler shift the AF reduces to the autocorrelation of $\tilde{s}(t)$

$$\chi(\tau,0) = \int_{-\infty}^{+\infty} \tilde{s}(t)\tilde{s}^*(t-\tau)\mathrm{d}t \tag{B.2}$$

B.1 Main Properties of the Ambiguity Function

The most important properties of the signal are presented below, assuming that the energy E of the signal s(t) is normalized.

1. The ambiguity function has a maximum at the origin (0,0) and can nowhere be higher.

$$\chi(\tau,\omega) \leq \chi(0,0) = 1 \tag{B.3}$$

2. The total volume of the ambiguity function is constant. It is notable that it is independent of the transmitted waveform.

$$\int_{-\infty}^{+\infty}\int_{-\infty}^{+\infty} \chi^2(\tau,\omega)\mathrm{d}\tau\mathrm{d}\omega = 1 \tag{B.4}$$

3. The ambiguity function is symmetric with respect to the origin.

$$\chi(\tau,\omega) = \chi(-\tau,-\omega) \tag{B.5}$$

B.2 Examples of the Ambiguity Function

The ideal ambiguity function is a single narrow spike at the origin with zero value elsewhere (fig.B.1). In this case the AF will achieve perfect range and Doppler resolution between targets even if they are located very close to each other, but an AF like this is impossible to create. This is because according to the aforementioned properties the AF must have finite peak value and volume.

- Single pulse Ambiguity function

The complex envelope of a normalized individual pulse is defined by:

$$\tilde{s}_1(t) = \frac{1}{\sqrt{T}}\mathrm{Rect}\left(\frac{t}{T}\right) \tag{B.6}$$

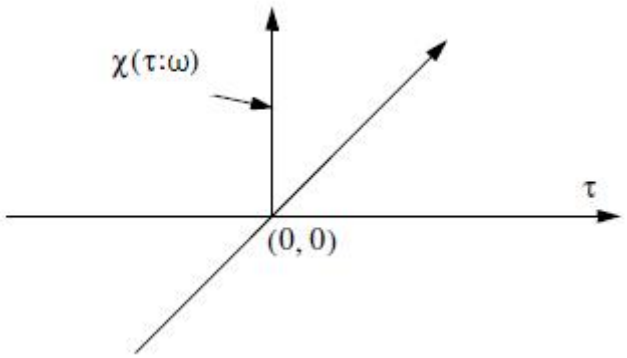

FIGURE B.1: Ideal Ambiguity Function.

Substituting Eq.(B.6) into Eq.(B.1) and performing the integration yield,

$$\chi(\tau,\omega) = \left(1 - \frac{|\tau|}{T}\right) \frac{\sin(\pi\omega(T-|\tau|))}{\pi\omega(T-|\tau|)} \ , \ \ |\tau| \leq T \tag{B.7}$$

Fig.B.2 and B.3 show the 3-D and the contour plots of the Ambiguity Function of a single pulse with pulse width of 3 seconds.

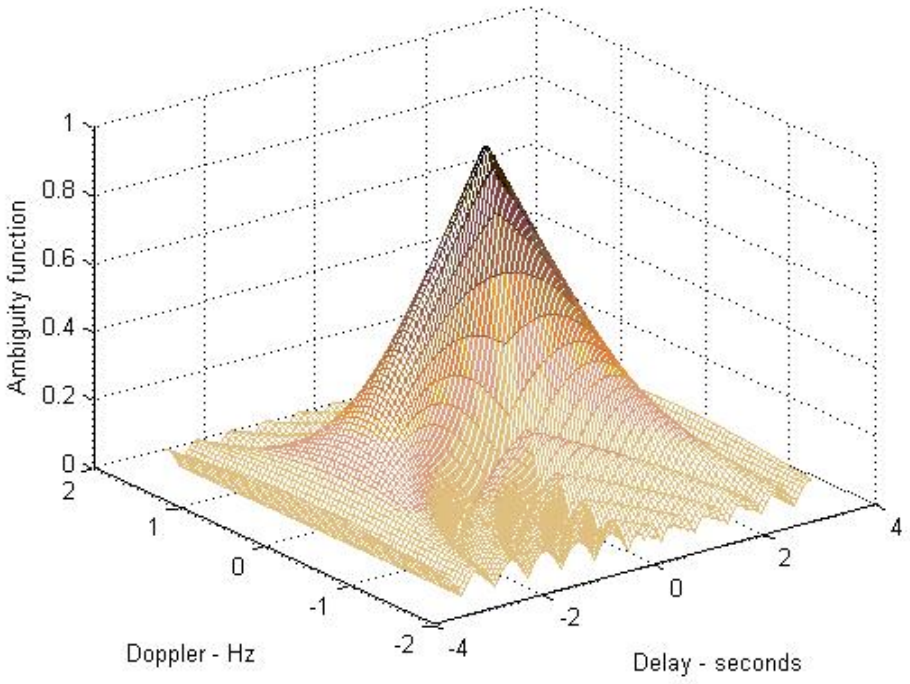

FIGURE B.2: 3-D plot of the single pulse Ambiguity Function.

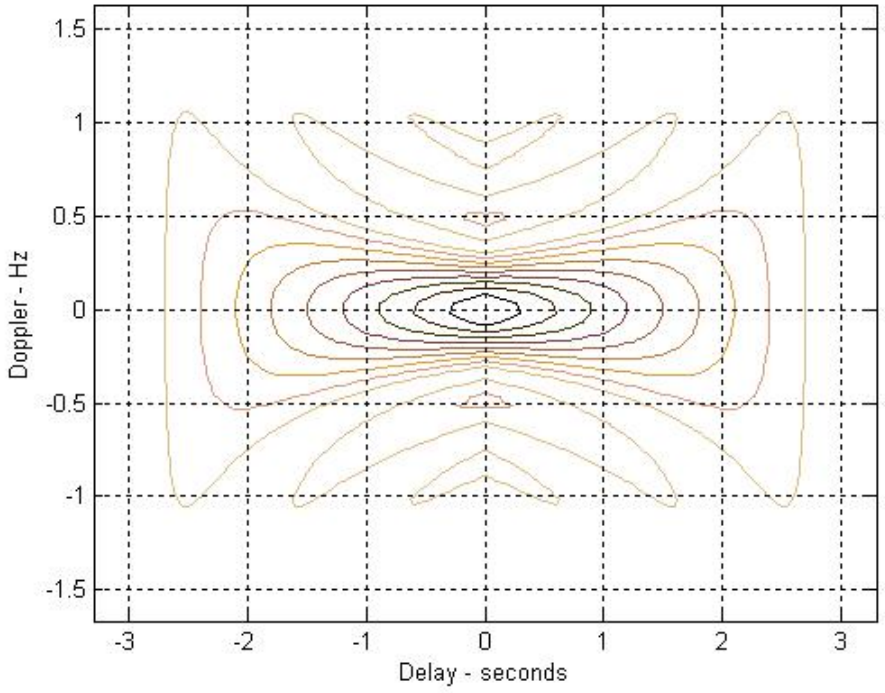

FIGURE B.3: Contour plot of the single pulse Ambiguity Function.

We can see that there is ambiguity in discriminating targets in both range and Doppler and we realize that in a single pulse range and Doppler resolutions are limited by the pulse duration. A satisfying range resolution could only be achieved by the transmission of a pulse with short duration but this leads to problems such as the use of large operating bandwidth and low transmitted power.

- LFM Ambiguity Function

As stated by Eq.(A.5) the complex envelope of an LFM waveform can be expressed by:

$$\tilde{s}(t) = \frac{1}{\sqrt{T}}\mathrm{Rect}\left(\frac{t}{\tau}\right)\exp\left[j\pi\mu t^2\right] \tag{B.8}$$

Substituting Eq.(B.8) into Eq.(B.1) and performing the integration yield,

$$\chi(\tau,\omega) = \left(1-\frac{|\tau|}{T}\right)\frac{\sin\left(\pi T(\mu\tau+\omega)\left(1-\frac{|\tau|}{T}\right)\right)}{\left(\pi T(\mu\tau+\omega)\left(1-\frac{|\tau|}{T}\right)\right)}\ ,\quad |\tau|\le T \tag{B.9}$$

Fig.B.4 and B.5 show the 3-D and the contour plots of the Ambiguity Function of a LFM single pulse with pulse width of 3 seconds and bandwidth of 5Hz.

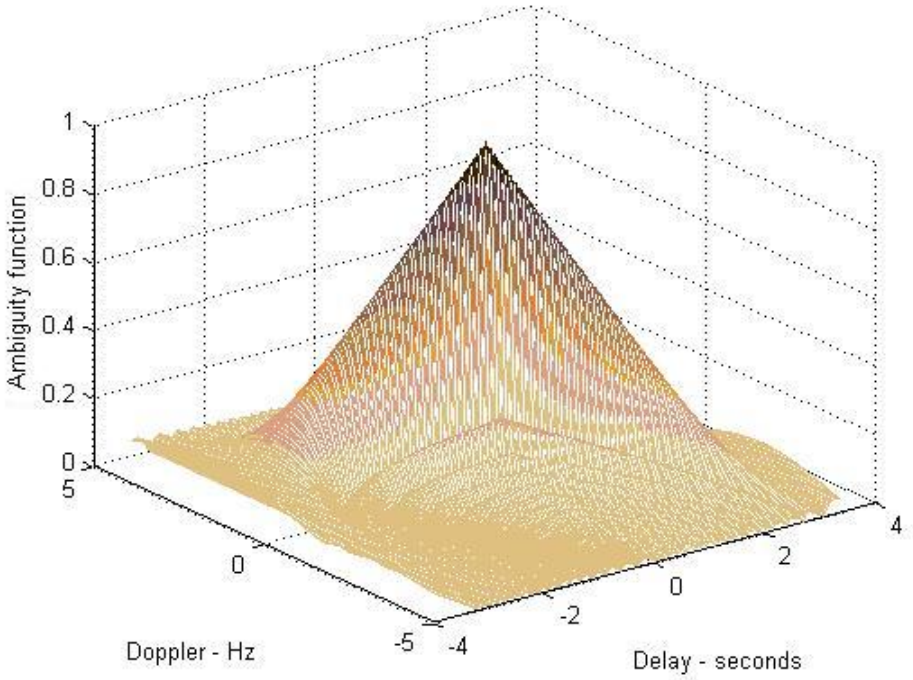

FIGURE B.4: 3-D plot of the LFM single pulse Ambiguity Function.

Figures B.4 and B.5 in comparison with figures B.2 and B.3 can clearly reveal the impact of the LFM on the ambiguity function of the single pulse. The AF forms a diagonal ridge on the Delay- Doppler map which gives us improved resolution in Delay and especially in Doppler.

- Coherent Train of Pulses Ambiguity Function

As stated by Eq.(A.7) a normalized train can be expressed by:

$$\tilde{s}(t) = \frac{1}{\sqrt{N}} \sum_{i=0}^{N-1} s_1(t - iT_{PRI}) \tag{B.10}$$

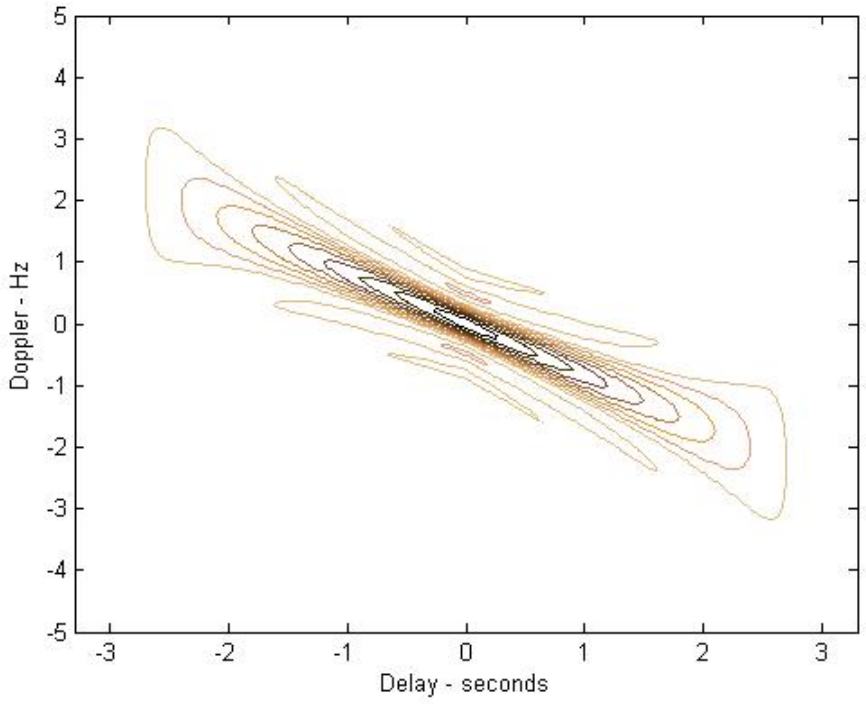

FIGURE B.5: Contour plot of the LFM single pulse Ambiguity Function.

where $\tilde{s}_1(t)$ is the normalized individual pulse defined by Eq.(A.6). Substituting Eq.(B.10) into Eq.(B.1) and performing the integration yield,

$$\chi(\tau,\omega) = \frac{1}{N}\sum_{q=-(N-1)}^{N-1}\chi_1(\tau - qT_{PRI},\omega)\frac{\sin(\pi\omega(N-|q|T_{PRI}))}{\sin(\pi\omega T_{PRI})}\ ,\ \ |\tau| \le NT_{PRI} \qquad \text{(B.11)}$$

where χ_1 is the Ambiguity Function of a single pulse.

Fig.B.6 and B.7 show the 3-D and the contour plots of the Ambiguity Function of a Coherent Train of Pulses of N=5, pulse width 0.2 seconds and T_{PRI} = 1 second. We notice the grid of recurrent lobes at intervals of T_{PRI} in delay and $1/T_{PRI}$ in Doppler, as a result of the superposition of the AFs of the separate pulses of the train. The appearance of the additional peaks in the AF surface of a Coherent Train of Pulses may result to unwanted range and Doppler uncertainties.

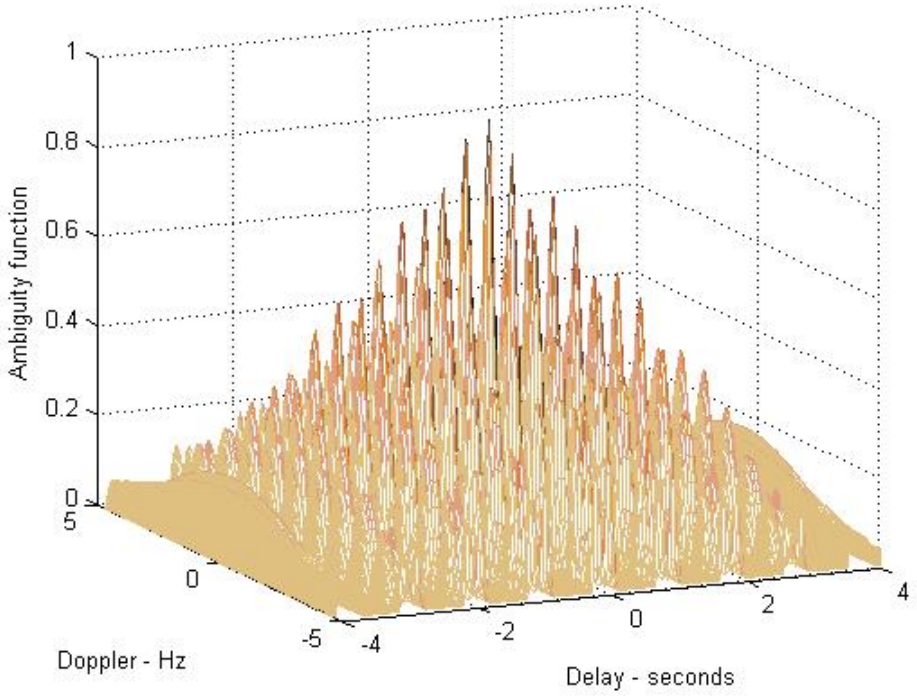

FIGURE B.6: 3-D plot of the LFM Coherent Train of Pulses Ambiguity Function.

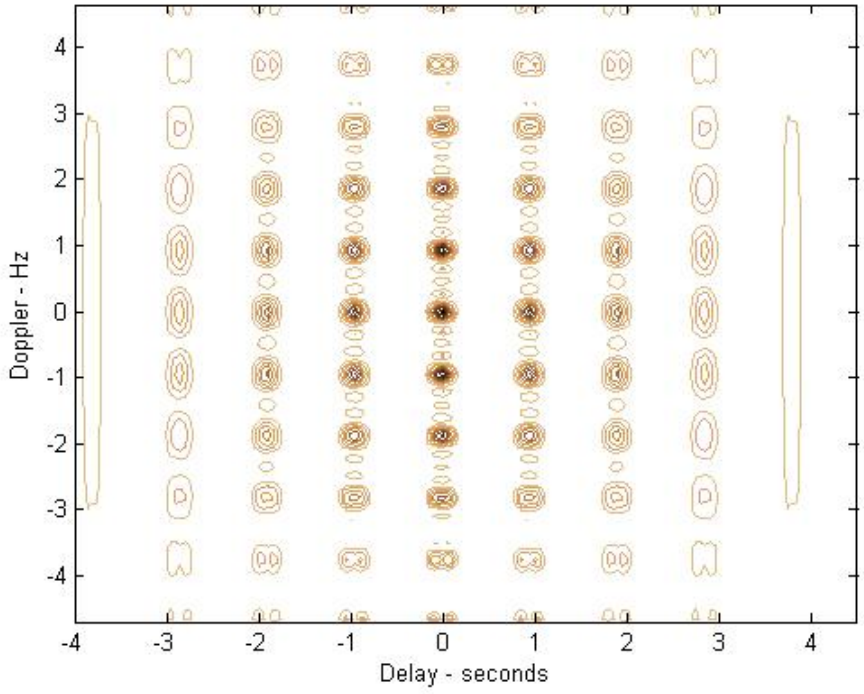

FIGURE B.7: Contour plot of the LFM Coherent Train of Pulses Ambiguity Function.

Bibliography

[1] Hans-Ulrich Schnitzler and Elisabeth KV Kalko. Echolocation by insect-eating bats we define four distinct functional groups of bats and find differences in signal structure that correlate with the typical echolocation tasks faced by each group. *Bioscience*, 51 (7):557–569, 2001.

[2] Jeanette A Thomas, Cynthia F Moss, and Marianne Vater. *Echolocation in bats and dolphins*. University of Chicago Press, 2004.

[3] Parthasarathy P Iyer. Designing of radar systems for passive detection and ranging: Target aquisition without transmission. In *Communication, Information & Computing Technology (ICCICT), 2012 International Conference on*, pages 1–6. IEEE, 2012.

[4] DKP Tan, Hong-bo Sun, Yi-long Lu, M Lesturgie, and HL Chan. Passive radar using global system for mobile communication signal: theory, implementation and measurements. In *Radar, Sonar and Navigation, IEE Proceedings-*, volume 152, pages 116–123. IET, 2005.

[5] Danny KP Tan, Hongbo Sun, and Yilong Lu. Sea and air moving target measurements using a gsm based passive radar. In *Radar Conference, 2005 IEEE International*, pages 783–786. IEEE, 2005.

[6] M. C. Wicks. Radar the next generation-sensors as robots. In *Radar Conference, 2003. Proceedings of the International*, pages 8–14. IEEE, 2003.

[7] Joseph R Guerci. Cognitive radar: a knowledge-aided fully adaptive approach. In *Radar Conference, 2010 IEEE*, pages 1365–1370. IEEE, 2010.

[8] National Institute of Mental Health. Definition of cognition. In *http://science.education.nih.gov/supplements/nih5/mental/other/glossary.htm*.

[9] Simon Haykin. Cognitive radar: a way of the future. *Signal Processing Magazine, IEEE*, 23(1):30–40, 2006.

[10] Constantino Rago, Peter Willett, and Yaakov Bar-Shalom. Detection-tracking performance with combined waveforms. *Aerospace and Electronic Systems, IEEE Transactions on*, 34(2):612–624, 1998.

[11] D. J. Kershaw and R. J. Evans. Optimal waveform selection for tracking systems. *Information Theory, IEEE Transactions on*, 40(5):1536–1550, 1994.

[12] BL Scala, Mohammad Rezaeian, and Bill Moran. Optimal adaptive waveform selection for target tracking. In *Information Fusion, 2005 8th International Conference on*, volume 1, pages 6–pp. IEEE, 2005.

[13] Krüger White, Jason Williams, and Peter Hoffensetz. Radar sensor management for detection and tracking. In *Information Fusion, 2008 11th International Conference on*, pages 1–8. IEEE, 2008.

[14] Ric A Romero and Nathan A Goodman. Cognitive radar network: Cooperative adaptive beamsteering for integrated search-and-track application. *Aerospace and Electronic Systems, IEEE Transactions on*, 49(2):915–931, 2013.

[15] A Aubry, A DeMaio, A Farina, and M Wicks. Knowledge-aided (potentially cognitive) transmit signal and receive filter design in signal-dependent clutter. *Aerospace and Electronic Systems, IEEE Transactions on*, 49(1):93–117, 2013.

[16] Dennis Wei and Alfred O Hero. Adaptive spectrum sensing and estimation. In *Acoustics, Speech and Signal Processing (ICASSP), 2013 IEEE International Conference on*, pages 5720–5724. IEEE, 2013.

[17] Michael Picciolo, Jacob D Griesbach, and Karl Gerlach. Adaptive lfm waveform diversity. In *Radar Conference, 2008. RADAR'08. IEEE*, pages 1–6. IEEE, 2008.

[18] Marco Piezzo, Antonio De Maio, Augusto Aubry, and Alfonso Farina. Cognitive radar waveform design for spectral coexistence. In *Radar Conference (RADAR), 2013 IEEE*, pages 1–4. IEEE, 2013.

[19] M La Manna, P Stinco, M Greco, and F Gini. Design of a cognitive radar for operation in spectrally dense environments. In *Radar Conference (RADAR), 2013 IEEE*, pages 1–6. IEEE, 2013.

[20] Lee K Patton and Brian D Rigling. Modulus constraints in adaptive radar waveform design. In *Radar Conference, 2008. RADAR'08. IEEE*, pages 1–6. IEEE, 2008.

[21] Wasim Huleihel, Joseph Tabrikian, and Reuven Shavit. Optimal adaptive waveform design for cognitive mimo radar. 2013.

[22] Hana Godrich, Athina P Petropulu, and Harold Vincent Poor. Power allocation strategies for target localization in distributed multiple-radar architectures. *Signal Processing, IEEE Transactions on*, 59(7):3226–3240, 2011.

[23] Phani Chavali and Arye Nehorai. Scheduling and power allocation in a cognitive radar network for multiple-target tracking. *Signal Processing, IEEE Transactions on*, 60(2): 715–729, 2012.

[24] Yogesh Nijsure, Yifan Chen, Said Boussakta, Chau Yuen, Yong Huat Chew, and Zhiguo Ding. Novel system architecture and waveform design for cognitive radar radio networks. *Vehicular Technology, IEEE Transactions on*, 61(8):3630–3642, 2012.

[25] Michele Vespe, Gareth Jones, and Chris J Baker. Lessons for radar. *Signal Processing Magazine, IEEE*, 26(1):65–75, 2009.

[26] Mary E Bates and James A Simmons. Perception of echo delay is disrupted by small temporal misalignment of echo harmonics in bat sonar. *The Journal of experimental biology*, 214(3):394–401, 2011.

[27] Marc W Holderied, Gareth Jones, and Otto von Helversen. Flight and echolocation behaviour of whiskered bats commuting along a hedgerow: range-dependent sonar signal design, doppler tolerance and evidence foracoustic focussing'. *Journal of Experimental Biology*, 209(10):1816–1826, 2006.

[28] Anthony E Petrites, Oliver S Eng, Donald S Mowlds, James A Simmons, and Caroline M DeLong. Interpulse interval modulation by echolocating big brown bats (eptesicus fuscus) in different densities of obstacle clutter. *Journal of Comparative Physiology A*, 195(6):603–617, 2009.

[29] Jianguo Ma and Rolf Müller. A method for characterizing the biodiversity in bat pinnae as a basis for engineering analysis. *Bioinspiration & biomimetics*, 6(2):026008, 2011.

[30] R Petrucci, S Immediata, L Timmoneri, and D Vigilante. Adaptive waveform generator for radar systems. In *Radar Conference, 2009. EuRAD 2009. European*, pages 573–576. IEEE, 2009.

[31] Mark R Bell and Chieh-Fu Chang. Frequency coded waveforms for adaptive waveform radar. In *Information Sciences and Systems, 2006 40th Annual Conference on*, pages 22–24. Citeseer, 2006.

[32] Chieh-Fu Chang and Mark R Bell. Frequency-coded waveforms for enhanced delay-doppler resolution. *Information Theory, IEEE Transactions on*, 49(11):2960–2971, 2003.

[33] Alessio Balleri, Hugh Griffiths, Marc Holderied, and Chris Baker. Bat-inspired multiharmonic waveforms. In *Waveform Diversity and Design Conference (WDD), 2010 International*, pages 000086–000089. IEEE, 2010.

[34] Martin Hurtado and Arye Nehorai. Bat-inspired adaptive design of waveform and trajectory for radar. In *Signals, Systems and Computers, 2008 42nd Asilomar Conference on*, pages 36–40. IEEE, 2008.

[35] Nathan A Goodman, Phaneendra R Venkata, and Mark A Neifeld. Adaptive waveform design and sequential hypothesis testing for target recognition with active sensors. *IEEE Journal of Selected Topics in Signal Processing*, 1(1):105, 2007.

[36] Yimin Wei, Huadong Meng, and Xiqin Wang. Adaptive single-tone waveform design for target recognition in cognitive radar. In *Radar Conference, 2009 IET International*, pages 1–4. IET, 2009.

[37] S. Suvorova, S.D. Howard, W. Moran, and R.J. Evans. Waveform libraries for radar tracking applications: Maneuvering targets. In *Information Sciences and Systems, 2006 40th Annual Conference on*, pages 1424–1428. IEEE, 2006.

[38] Yifan Chen, Yogesh Nijsure, Chau Yuen, Yong Huat Chew, Zhiguo Ding, and Said Boussakta. Adaptive distributed mimo radar waveform optimization based on mutual information. *Aerospace and Electronic Systems, IEEE Transactions on*, 49(2):1374–1385, 2013.

[39] Junhyeong Bae and Nathan A Goodman. Automatic target recognition with unknown orientation and adaptive waveforms. In *Radar Conference (RADAR), 2011 IEEE*, pages 1000–1005. IEEE, 2011.

[40] M. R. Bell. Information theory and radar waveform design. *Information Theory, IEEE Transactions on*, 39(5):1578–1597, 1993.

[41] Bin Wang, Jinkuan Wang, Xin Song, and Yinghua Han. A new waveform design method for cognitive radar. In *Proceedings of the 3rd international conference on Intelligent information technology application*, pages 176–179. IEEE Press, 2009.

[42] Wasim Huleihel, Joseph Tabrikian, and Reuven Shavit. Optimal sequential waveform design for cognitive radar. In *Acoustics, Speech and Signal Processing (ICASSP), 2012 IEEE International Conference on*, pages 2457–2460. IEEE, 2012.

[43] Anish Turlapaty and Yuanwei Jin. Parameter estimation and waveform design for cognitive radar by minimal free-energy principle. In *Acoustics, Speech and Signal Processing (ICASSP), 2013 IEEE International Conference on*, pages 6244–6248. IEEE, 2013.

[44] Philipp M Woodward. Probability and information theory. 1953.

[45] Simon Haykin, Amin Zia, Ienkaran Arasaratnam, and Yanbo Xue. Cognitive tracking radar. In *Radar Conference, 2010 IEEE*, pages 1467–1470. IEEE, 2010.

[46] Zhang Zhen-kai, Zhou Jian-jiang, and Wang Fei. An algorithm of target tracking based on adaptive lfm waveform design. In *Advanced Computer Control (ICACC), 2010 2nd International Conference on*, volume 5, pages 130–132. IEEE, 2010.

[47] Phani Chavali and Arye Nehorai. Cognitive radar for target tracking in multipath scenarios. In *Waveform Diversity and Design Conference (WDD), 2010 International*, pages 000110–000114. IEEE, 2010.

[48] Tianyao Huang, Yimin Liu, Huadong Meng, and Xiqin Wang. Adaptive waveform design in random stepped frequency radar. *International Radar Conference, IET*, 1(1): 221, 2013.

[49] Guan Zhai, Huadong Meng, and Xiqin Wang. Adaptive pri selection for tracking in clutter. *International Radar Conference, IET*, 1(1):314, 2013.

[50] Sandeep P Sira, Douglas Cochran, Antonia Papandreou-Suppappola, Darryl Morrell, William Moran, Stephen D Howard, and Robert Calderbank. Adaptive waveform design for improved detection of low-rcs targets in heavy sea clutter. *Selected Topics in Signal Processing, IEEE Journal of*, 1(1):56–66, 2007.

[51] Feng Jiang, Jie Chen, and A Lee Swindlehurst. Linearly reconfigurable kalman filtering for a vector process. In *Acoustics, Speech and Signal Processing (ICASSP), 2013 IEEE International Conference on*, pages 5725–5729. IEEE, 2013.

[52] Ienkaran Arasaratnam and Simon Haykin. Cubature kalman filters. *Automatic Control, IEEE Transactions on*, 54(6):1254–1269, 2009.

[53] Yaakov Bar-Shalom. Multitarget-multisensor tracking: advanced applications. *Norwood, MA, Artech House, 1990, 391 p.*, 1, 1990.

[54] Zhen Ding and Bhashyam Balaji. Comparison of the unscented and cubature kalman filters for radar tracking applications. In *Radar Systems (Radar 2012), IET International Conference on*, pages 1–5. IET, 2012.

[55] G.G.V. Morris and L.L. Harkness. *Airborne Pulsed Doppler Radar*. Radar Library. Artech House, Incorporated, 1996. ISBN 9780890068670.

[56] Nil Garcia, Alexander M Haimovich, Martial Coulon, and Marco Lops. Resource allocation in mimo radar with multiple targets for non-coherent localization. *arXiv preprint arXiv:1308.6543*, 2013.

[57] R Tharmarasa, T Kirubarajan, A Sinha, and T Lang. Decentralized sensor selection for large-scale multisensor-multitarget tracking. *Aerospace and Electronic Systems, IEEE Transactions on*, 47(2):1307–1324, 2011.

[58] John D Glass and LD Smith. Mimo radar resource allocation using posterior cramér-rao lower bounds. In *Aerospace Conference, 2011 IEEE*, pages 1–9. IEEE, 2011.

[59] Yuan Shen, Wenhan Dai, and Moe Z Win. Optimal power allocation for active and passive localization. In *Global Communications Conference (GLOBECOM), 2012 IEEE*, pages 3713–3718. IEEE, 2012.

[60] Edin Insanic and Paul Siqueira. Use of vector velocity estimate accuracy for improved resource allocation in a network of doppler radars. In *Geoscience and Remote Sensing Symposium, 2008. IGARSS 2008. IEEE International*, volume 3, pages III–1123. IEEE, 2008.

[61] Chen Ming Yan and Wang Lei. Resource management algorithm based on the minimum covariance mean deviation criterion for phased array radars. In *Microwave and Millimeter Wave Circuits and System Technology (MMWCST), 2012 International Workshop on*, pages 1–4. IEEE, 2012.

[62] Gregory E Newstadt, Edmund G Zelnio, and Alfred O Hero. Adaptive resource allocation for synthetic aperture radars under resource constraints. In *SPIE Defense, Security, and Sensing*, pages 87460F–87460F. International Society for Optics and Photonics, 2013.

[63] PJ Fielding and AM Kinghorn. Waveform optimisation for efficient resource allocation in airborne aesa radar systems. In *Multifunction Radar and Sonar Sensor Management Techniques (Ref. No. 2001/173), IEE*, pages 3–1. IET, 2001.

[64] Ayhan Irci, Afsar Saranli, and Buyurman Baykal. Study on q-ram and feasible directions based methods for resource management in phased array radar systems. *Aerospace and Electronic Systems, IEEE Transactions on*, 46(4):1848–1864, 2010.

[65] Jinwoo Seok, Jinxin Zhao, Jhanani Selvakumar, Edwin Sanjaya, Pierre T Kabamba, and Anouck Girard. Radar resource management: Dynamic programming and dynamic

finite state machines. In *Control Conference (ECC), 2013 European*, pages 4100–4105. IEEE, 2013.

[66] John Ostwald, Victor Lesser, and Sherief Abdallah. Combinatorial auctions for resource allocation in a distributed sensor network. In *Real-Time Systems Symposium, 2005. RTSS 2005. 26th IEEE International*, pages 9–pp. IEEE, 2005.

[67] RP Singh. Solving 0–1 knapsack problem using genetic algorithms. In *Communication Software and Networks (ICCSN), 2011 IEEE 3rd International Conference on*, pages 591–595. IEEE, 2011.

[68] Christine Solnon and Derek Bridge. An ant colony optimization meta-heuristic for subset selection problems. *System Engineering using Particle Swarm Optimization, Nova Science*, pages 7–29, 2006.

[69] Zhi Tian, Geert Leus, and Vincenzo Lottici. Joint dynamic resource allocation and waveform adaptation in cognitive radio networks. In *Acoustics, Speech and Signal Processing, 2008. ICASSP 2008. IEEE International Conference on*, pages 5368–5371. IEEE, 2008.

[70] Sergio Miranda, Chris Baker, Karl Woodbridge, and Hugh Griffiths. Knowledge-based resource management for multifunction radar: a look at scheduling and task prioritization. *Signal Processing Magazine, IEEE*, 23(1):66–76, 2006.

[71] Nadav Levanon and Eli Mozeson. *Radar signals*. John Wiley & Sons, 2004.

[72] John P Costas. A study of a class of detection waveforms having nearly ideal range—doppler ambiguity properties. *Proceedings of the IEEE*, 72(8):996–1009, 1984.